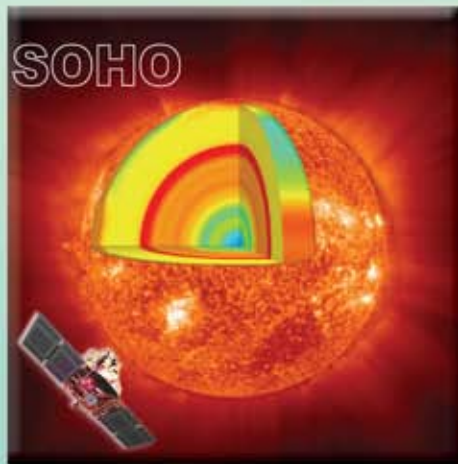
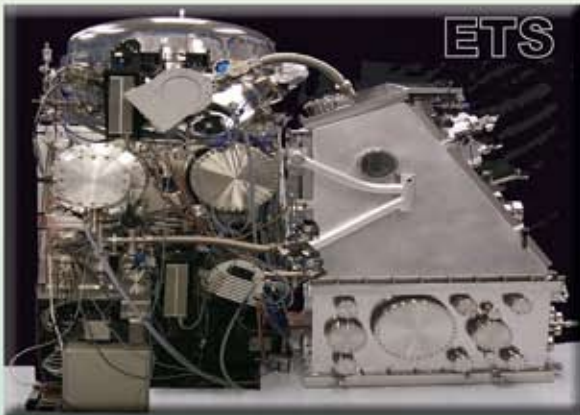


AXUV/SXUV/UVG



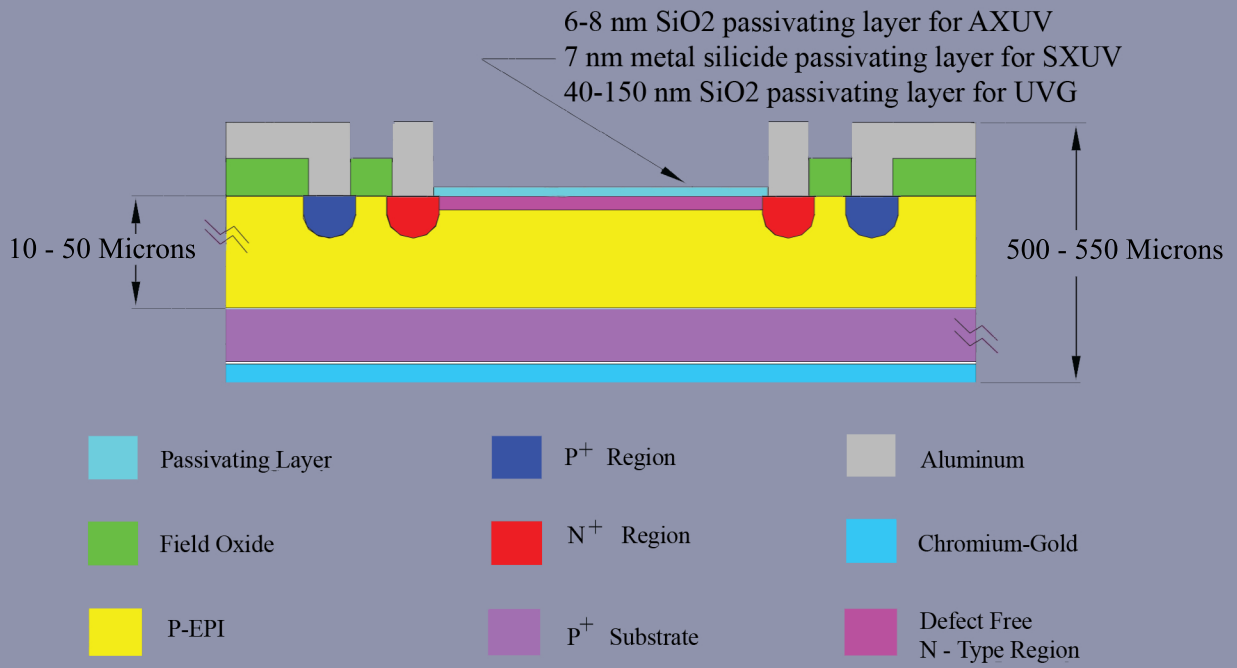
Salient Applications



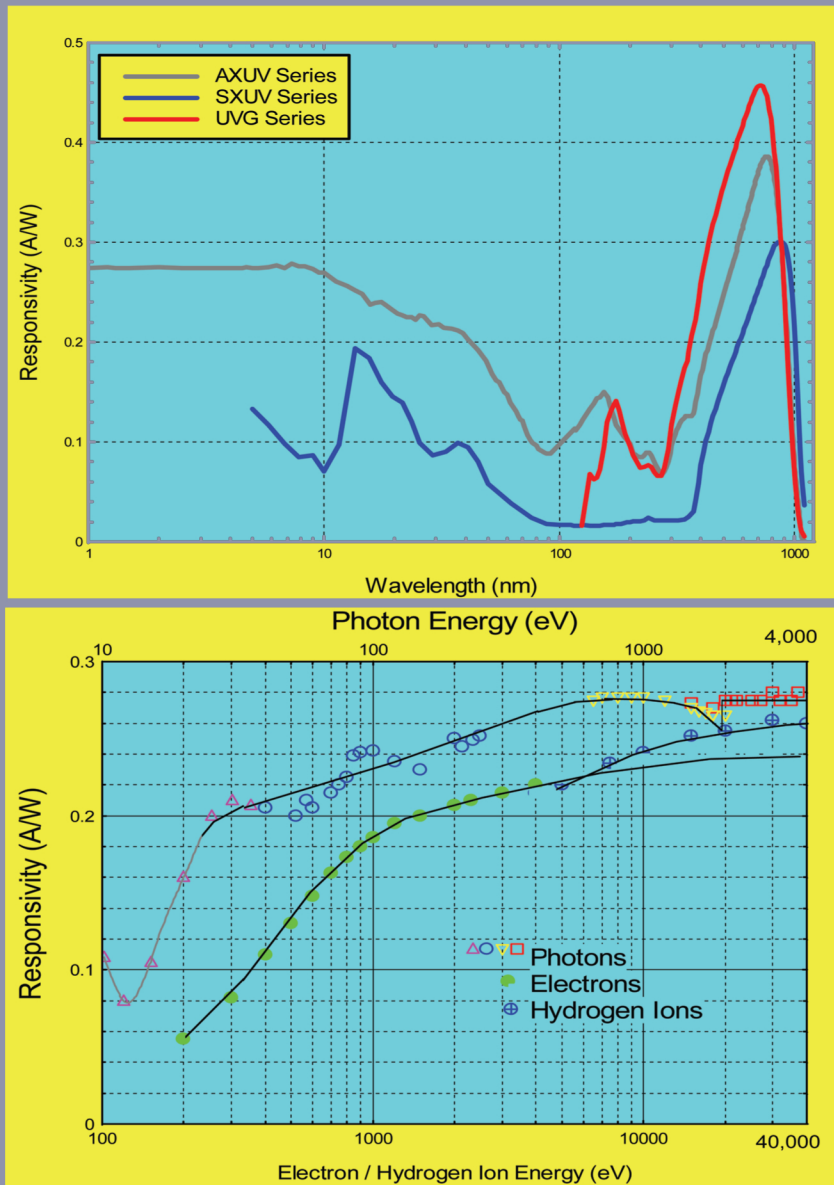
INTERNATIONAL RADIATION DETECTORS, INC.
2527 West 237th St. Unit A Torrance, California 90505-5243
Phone: (310) 534-3661 web: <http://www.ird-inc.com>
Fax: (310) 534-3665 email: sales@ird-inc.com



Advancing the UV/EUV Measurement Science



Structure of the AXUV, SXUV and UVG Photodiodes



CONTENTS

1) Introduction.....	1	14) High Energy x-rays.....	9
2) Photodiode Selection.....	1	15) Applications.....	9
3) Quantum Efficiency.....	1	16) Radiometric Characterization.....	10
4) CW Responsivity.....	3	17) References.....	11
5) Pulse Responsivity.....	3	18) Diodes with Integrated Bandpass Filters.....	12
6) Responsivity Stability.....	4	19) Standard Products.....	13
7) Spatial Responsivity Uniformity.....	5	I) AXUV devices	
8) Temperature Dependence.....	6	II) SXUV devices	
9) Linearity / Dynamic Range.....	7	III) UVG devices	
10) Noise Characteristics.....	7	20) Package Drawing.....	17
11) Time Response.....	8	21) Ceramic and Teflon Sockets.....	25
12) Polarization Sensitivity.....	8	22) Electronics.....	29
13) Proper Use.....	8	I) BT 250 Bias Tee	
		II) PA 100 Amplifier	
		III) PA 13 Amplifier	
		IV) AXUV100HYB1/V	
		V) AXUV16ELOHYB1	
		VI) AMP16	
		VII) QSP1	

Introduction:

Silicon p-n junction photodiodes have been developed by International Radiation Detectors Inc. for the detection of UV, EUV and x-ray (wavelength range 1100 nm to .0124 nm, energy range 1.12 eV to 100 KeV) photons and low energy electrons and ions. IRD Manufactures AXUV, SXUV, and UVG series diodes to cover some of these applications. The photodiodes are fabricated by an ULSI (Ultra Large Scale Integrated Circuit) compatible process and their construction is shown in the top figure on the left page. Unlike common p-n junction diodes, the AXUV/UVG series photodiodes do not have a doped dead-region in the front and have zero surface recombination resulting in near theoretical quantum efficiencies for UV/XUV photons and other low energy particles. SXUV series photodiodes have been specifically developed for photon detection with high flux levels like those encountered in third and fourth generation synchrotrons and excimer lasers.

Photodiode Selection:

Photodiode users are requested to select the optimum devices for their applications as follows:

1) AXUV (Absolute XUV) series devices can be used to cover the complete photon spectral range (0.0124 nm to 1100 nm) and should be used for detection of low energy electrons and ions because of their 6 nm oxide window and 100% internal quantum efficiency $\{Q(\epsilon_{ph})\}$.

2) Because the oxide window will create surface recombination (resulting in loss of 100% internal quantum efficiency) after receiving several G-rad (SiO_2) dose, SXUV series diodes with metal silicide window have been developed. These diodes have almost infinite radiation hardness to photons. Owing to this feature, SXUV series diodes are recommended when high photon flux is involved and for detection of UV/EUV pulse radiation when the pulse energy density is higher than $0.1 \mu\text{J}/\text{cm}^2$.

3) Like the AXUV series diodes, UVG series diodes have 100% internal quantum efficiency. The oxide window on these devices is 70 to 150 nm thick which is optimized for 140 nm to 1100 nm photon detection.

Quantum Efficiency:

When the silicon photodiode is exposed to photons with energy greater than 1.12 eV (wavelength less than 1100 nm), electron-hole pairs (carriers) are created. These photogenerated carriers are separated by the p-n junction electric field and a current proportional to the number of electron-hole pairs created flows through an external circuit. Ultraviolet photons, with wavelength shorter than about 350 nm, create more than one electron-hole pair [1]. This results in internal quantum efficiencies greater than unity as shown in Fig 1.

Several unique properties of the AXUV/UVG photodiodes have resulted in previously unattained stability and 100%

carrier collection efficiencies giving rise to near theoretical quantum efficiencies.

The first property is the absence of a surface dead region i.e. no photogenerated carrier recombination occurs in the doped n-type region and at the silicon-silicon dioxide interface. As the absorption depths for the majority of UV/EUV photons are less than 1 micrometer in silicon, the absence of a dead region yields complete collection of photogenerated carriers by an external circuit resulting into 100% collection efficiency. Fig. 1 shows that these diodes have 100% collection efficiency in 350 nm to 640 nm spectrum region, and higher at shorter wavelength.

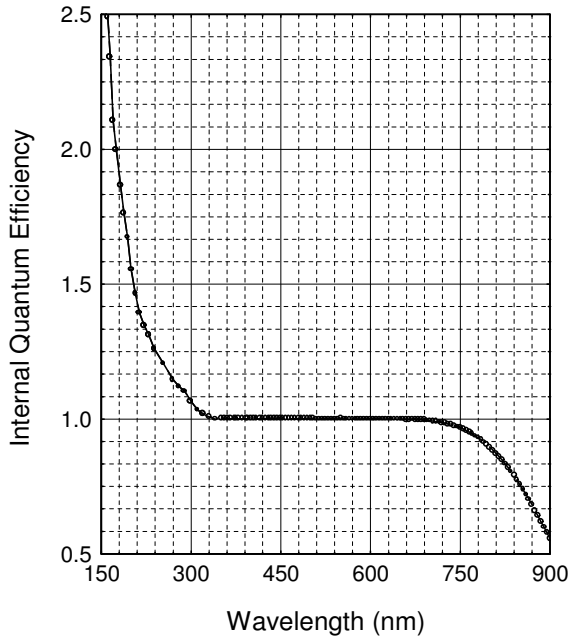


Fig. 1: Internal quantum efficiency of the AXUV/UVG photodiodes.

Recently, 1 cm² active area UVG100 diodes were used to determine quantum yield (number of electron-hole pairs generated per absorbed photon) of silicon in 254 nm to 160 nm spectral region [2]. Quantum yield in this region was determined for the first time using the UVG100 diodes and is shown in Fig. 1 from 320 nm to 150 nm.

This quantum yield knowledge now makes possible development of trap detectors for absolute flux determination in applications like deep UV lithography, and photorefractive and phototherapeutic keratectomy. Owing to their 100% collection efficiency, the external quantum efficiency of UVG photodiodes can be calculated in the UV and short wavelength visible (about 160 nm to 640 nm) as the product of the internal quantum efficiency times one minus the reflectance of the photodiode. The internal quantum efficiency can be taken from Fig. 1 and the reflectance can be measured or calculated. Fig. 2 shows the measured reflectance from 150 nm to 1100 nm for the UVG series photodiodes with 70 nm oxynitride front window.

As the UVG series diode internal quantum efficiency drops rapidly after 700 nm owing to the limited silicon thickness, IRD also provides p-on-n photodiodes (for example: UVGPN100, UVGPN20, etc.) which have shown over 97% internal quantum efficiency at 950 nm.

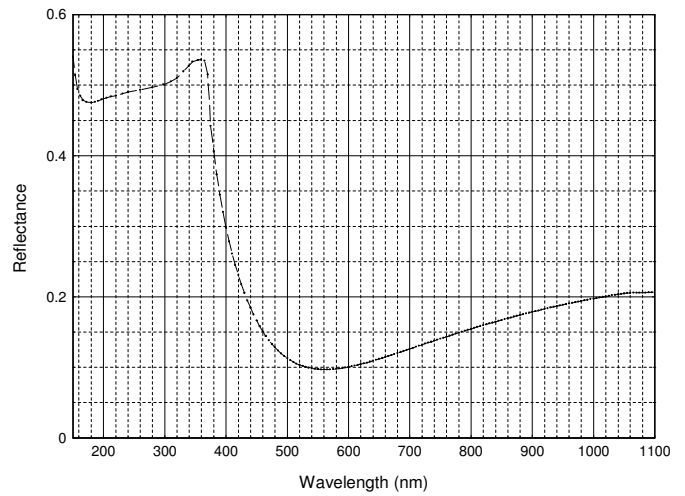


Fig. 2: Typical reflectance of UVG photodiodes.

The second unique property of the AXUV diodes is their extremely thin (4 to 8 nm), radiation-hard silicon dioxide junction passivating, protective entrance window. Owing to their 100% collection efficiency and the thin entrance window, the quantum efficiency of the AXUV diodes can be approximately predicted in most of the XUV region by the theoretical expression $\epsilon_{ph}/3.65$, where ϵ_{ph} is the photon energy in electron-volts. The only quantum efficiency loss is due to the front (4 to 8 nm) silicon dioxide window at wavelengths for which oxide absorption (mainly for 8 to 100 eV photons) and reflection are not negligible. Fig. 3 shows the typical quantum efficiency plot of AXUV photodiodes.

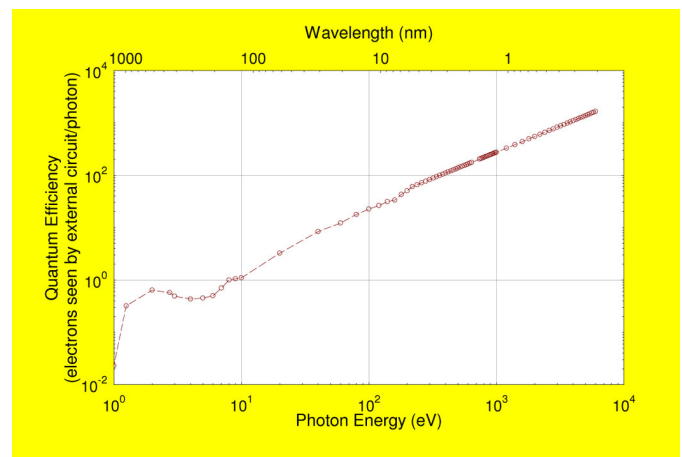


Fig. 3: Typical quantum efficiency of AXUV photodiodes.

CW Responsivity:

Center figure on the front inside cover shows typical CW responsivity of the AXUV/SXUV/UVG photodiodes. As the responsivity is quantum efficiency divided by the corresponding photon energy, the AXUV photodiode responsivity can also be calculated from Fig. 3. Note that the AXUV responsivity has the theoretical value of 0.275 A/W for short wavelength photons.

As seen in the figure, responsivity of the SXUV photodiodes is significantly lower than the responsivity of the AXUV series diodes due to the surface recombination present in these devices.

Owing to their extremely thin (4 to 8 nm) entrance window, AXUV diodes exhibit near theoretical response to low energy electrons and hydrogen ions. The bottom figure on the front inside cover shows the responsivity of AXUV photodiodes to photons with 10 eV to 4000 eV energy and to electrons and hydrogen ions with 100 eV to 40,000 eV energy [3-5]. Figure 4 shows the same information in terms of gain for 80 eV to 40,000 eV electrons.

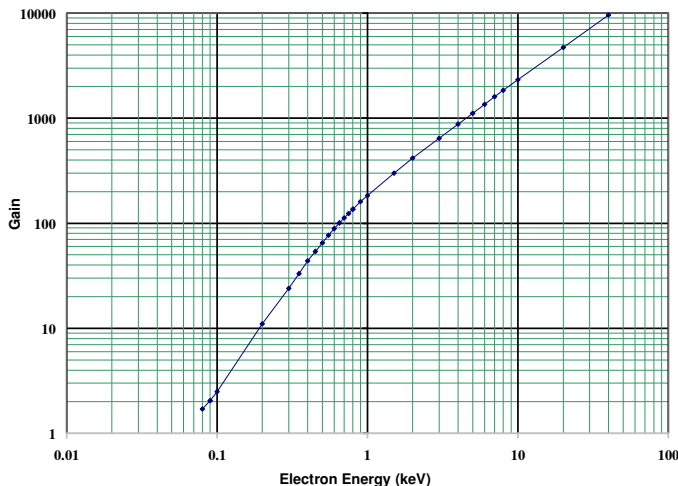


Fig. 4: Gain of the AXUV photodiodes to electrons.

Pulse Responsivity:

Table 1 gives the 193nm pulse and CW responsivity for the SXUV100 and UVG100 diodes. An MPB 193 nm excimer laser (model # PSX100) was used to measure the pulse responsivity. The pulse duration of the PSX100 is 10 ns. Attenuators were used to reduce the 3 mJ pulse energy of the PSX100 to the pulse energies shown in Table 1. A capacitively coupled bias tee (IRD model BT250) was used to reverse bias the detectors up to 120 V. The photodiode voltage as a function of time $V(t)$ was measured with a LeCroy 500 MHz digital oscilloscope with 50 ohm input impedance R .

The charge Q created in the photodiode per pulse was calculated as:

$$Q = (1/R) \int V dt$$

This integral was evaluated using the oscilloscope's built-in area function. The pulse energy of the PSX100 was measured with an Ophir Laserstar with PE10 pyroelectric detector head which has an uncertainty of approximately 10% with 2 μ J incident pulse energy at 193 nm.

The pulse responsivity (charge generated per unit energy incident) was calculated by dividing the measured charge created in the detector by the measured pulse energy. As seen in Table 1, the correlation between the cw and pulsed 193 nm response agrees with previous results for visible wavelengths [6]. This experimental verification that the cw responsivity can be used to measure pulse energy is critical to radiometric measurements of 13 nm pulses for which no primary standards are presently available.

As the UV/EUV, light pulses are very destructive to sensors because of the high flux levels involved, SXUV photodiodes were developed specifically for sources with high flux levels to yield years of operation without noticeable degradation.

Unlike pyroelectric detectors which have only five to six orders of magnitude dynamic range and a significant non-uniformity of response across the surface, SXUV series photodiodes have over nine orders of magnitude dynamic range with non-uniformity less than $\pm 2\%$. The solid state accuracy and reliability as well as the compact size and low cost of the SXUV photodiodes will provide an effective replacement for pyroelectric detectors in some applications.

To operate SXUV photodiodes with over 9 decades of linear range, IRD has developed the PA100 pulse amplifier for use with a digital oscilloscope. This amplifier, when used in combination with the SXUV series photodiodes, will provide a means to measure pulse energies lower than 1 pJ. The specifications of the PA100 amplifier are shown on page 27.

The SXUV100RPD photodiode was specifically developed to measure UV pulse energies up to 100 μ J. Bottom figure on the back cover shows the linear range of SXUV100RPD photodiode at 150 volts bias with BT250 bias T. The PA100 amplifier was used to measure the 193 nm pulse energies below 10 nJ with 10 volts bias on the detector.

For EUV pulse detection with mJ pulse energies, the SXUV100mj device was developed. Unlike the flying circus and other experimental EUV energy measurement schemes, the SXUV100mj diodes do not use any front-mounted mirrors. The SXUV diode utilizes a directly deposited filter with a passband of 12.2 to 15.8 nm (see page 12, SXUV100Mo/Si). A 100 nm thick paralyne and 20 nm Al filter absorbs infrared radiation emitted from the SS mesh shown in the package 100mj on page 22.

		Responsivity for 193 nm Pulse Radiation					
		100 V Reverse Bias			120 V Reverse Bias		
Device	CW Responsivity @ 193 nm	100 nJ	1 μ J	2.5 μ J	100 nJ	1 μ J	2.5 μ J
UVG100 00-26	.137 A/W	.127 C/J	.122 C/J	sat	.129 C/J	.123 C/J	sat
SXUV100 02-2	.0104 A/W	.0101 C/J	.0108 C/J	.0105 C/J	.0102 C/J	.0108 C/J	.0105 C/J

Table 1: Comparison of CW and pulse responsivity of UVG and SXUV series photodiodes when exposed to 100 nJ, 1 μ J and 2.5 μ J pulses with a 3 mm diameter beam. Because of the high responsivity, the UVG diode was saturated at the 2.5 μ J/pulse energy level [7].

Responsivity Stability:

It is known that the UV/EUV photon exposure induced instability of common silicon photodiodes is caused by the front silicon dioxide window [1]. IRD photodiodes have been developed to have unparalleled radiation hardness by optimization of the front window.

The radiation hardness of AXUV diodes is 100 to 1,000 Mrads (SiO₂) when tested with 10 eV photons. This hardness is about 10,000 times greater than that of commonly available PIN silicon photodiodes.

Diodes with 1 Gigarad (SiO₂) hardness are fabricated by nitrogen doping at the Si-SiO₂ interface to form an oxynitride window instead of the common silicon dioxide window [8]. The letter G at the end of a model number indicates this type of device. The 1 Gigarad (SiO₂) hardness achieved is the highest hardness ever reported or known to exist in any silicon device.

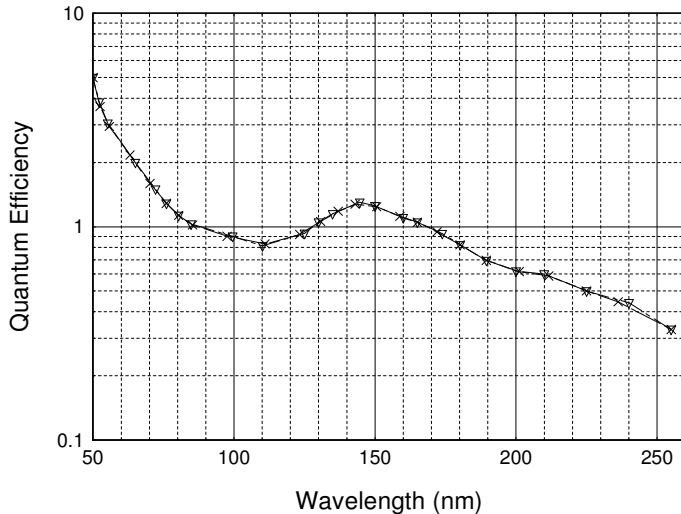


Fig. 5: Quantum efficiency of AXUV photodiodes with 60 Å oxynitride passivating front window. Δ -Before exposure, \times -after exposure to 100% relative humidity for 4 weeks [8].

To minimize the effects of quantum efficiency instability mechanisms, AXUV/UVG photodiodes are fabricated in an extremely clean environment to have negligible latent recombination centers and a trap-free, moisture insensitive Si-SiO₂ interface. Nitrogen incorporation in the Si-SiO₂ interface

is known to make it insensitive to impurity penetration [8]. Figure 5 shows a quantum efficiency plot of the AXUV G series diodes before and after exposure to 100% relative humidity. These diodes were fabricated by nitrogen incorporation at the interface and hence have exhibited no change in the 50 to 250 nm quantum efficiency even after 4 weeks of 100% relative humidity exposure at room temperature.

International laboratories like NIST and PTB have already approved use of AXUV silicon photodiodes as transfer standards. In fact, AXUV100G diodes are being used by some scientists as absolute detectors in the 30 eV to 6 keV range using the self-calibration process. The uncertainty, as reported by PTB scientists [9], in the self-calibration process is $\pm 4\%$, while the orthodox secondary standards used in this range may have calibration uncertainties over $\pm 10\%$. Thus, the use of the AXUV diodes for absolute radiometry is quite attractive.

The radiation hard, junction passivating, oxynitride protective entrance window of the UVG series diodes makes them extremely stable after exposure to intense flux of UV photons. They show less than 2% responsivity degradation after megajoules/cm² of 254 nm and tens of kilojoules/cm² of 193 nm photon exposure. Because the UVG photodiodes do not show any degradation due to moisture exposure, they are typically used without a quartz protective window. This open face configuration is extremely advantageous in applications where quartz window interference effects are problematic.

As n-on-p diodes are more radiation-hard than the more common p-on-n devices [10,11], UVG and the AXUV diodes are better suited for space missions. 4 mm and 5 mm diameter active area UVG diodes are being used in the Multi-Angle Imaging Spectro Radiometer (MISR) as part of NASA’s Earth observing system [12]. These devices are also being used aboard an Argentinean satellite.

As pointed out in the photodiode selection section, the passivating SiO₂ window of the AXUV/UVG series diodes will create surface recombination after receiving several Gigarad (SiO₂) dose resulting in loss of quantum efficiency. The metal silicide window in the SXUV series diodes replaces the standard SiO₂ window eliminating the UV/EUV exposure induced instability problem [6,13]. Stability tests performed on the SXUV diodes with 244 nm CW laser with 8.5 W/cm²

power density (1.5 mm diameter spot, 150 mW beam power) show about 4.5% increase in the 244 nm responsivity after 4 days of exposure. As this increased responsivity did not decrease after 5 months of storage in nitrogen, it is presumed that the increased responsivity is caused by surface cleaning effects due to the high intensity laser beam. Top figure on the back cover, shows that the SXUV diodes exhibit less than 2% change in responsivity after receiving one billion 100 $\mu\text{J}/\text{cm}^2$ pulses from both 193 nm and 157 nm excimer lasers.

Fig. 6 shows the responsivity stability of the SXUV100 diode compared to the AXUV100G diode when exposed to 100 eV photons with 3×10^{14} photons/sec/cm² (5 mW/cm²) flux. The beam size used was 0.1 mm x 0.5 mm. After receiving a total fluence of 1.8×10^{18} photons/cm² (29 J/cm²), the AXUV100G diode showed approximately 28 % decrease in response while the SXUV100 diode showed virtually no change after the same exposure. Further exposure indicated that no change in the SXUV100 diode responsivity is noticed after receiving a total fluence of 10^{22} photons/cm² (160kJ/cm²) [7,14]. Fig. 5 also shows responsivity stability of the AXUV100G diode when exposed to 10 eV photons with 5×10^{13} photons/sec/cm² (80 $\mu\text{W}/\text{cm}^2$) flux. Again, virtually no change in the SXUV100 diode responsivity was noticed after several hours of this exposure.

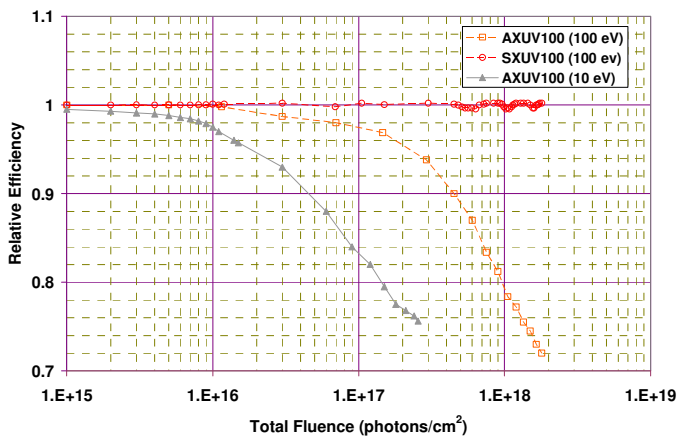


Fig. 6: Relative responsivity of SXUV100 and AXUV100G photodiodes when exposed to 100eV and 10eV photons.

Fig. 7 shows a scan of the SXUV100 detector surface before and after exposure to 100eV photons with a fluence in excess of $10^{22}/\text{cm}^2$. The arrow indicates the position where the detector was exposed to the synchrotron radiation beam for several hours. Taking into account the measurement uncertainty, it may be concluded that there is no change in the diode responsivity after receiving the above fluence. Note also that uniformity of the SXUV100 diodes is within a couple of percent when scanned with the 0.1 mm x 0.5 mm beam.

The majority of the SXUV series diodes have a nitrided titanium silicide front window because of the excellent information available in the literature [15]. However, SXUV

diodes with platinum silicide front windows can be supplied upon special request.

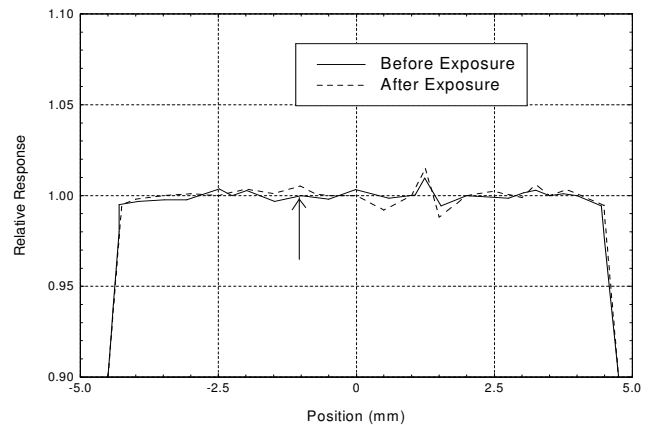


Fig. 7: Line scan of the SXUV100 diode with 12.4 nm beam before and after exposure to 10^{22} photons/cm² 100 eV photons.

Spatial Responsivity Uniformity:

Figures 8 and 9 show the spatial responsivity uniformity for the AXUV100G photodiode at 160.4 nm and 121.6 nm respectively. It is interesting to note that the uniformity at 160.4 nm is better than that at 121.6 nm. Since the AXUV photodiodes have 100% internal quantum efficiency; this difference in uniformity is apparently caused by a slightly non-uniform oxide thickness. As 121.6 nm photons are more readily absorbed in SiO₂ than 160.4 nm photons, non-uniformities in the oxide will have a larger effect on spatial response uniformity at 121.6 nm than at 160.4 nm. This suggests that any desired improvement in the spatial responsivity uniformity will require improved fabrication techniques to grow more uniform thin oxides.

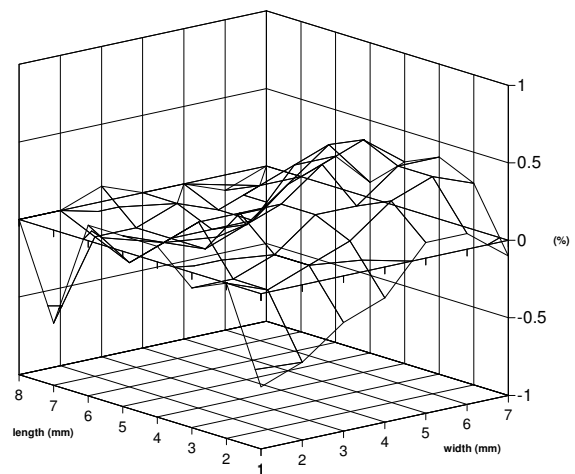


Fig. 8: Spatial responsivity uniformity of the AXUV100G photodiode at 160.4 nm.

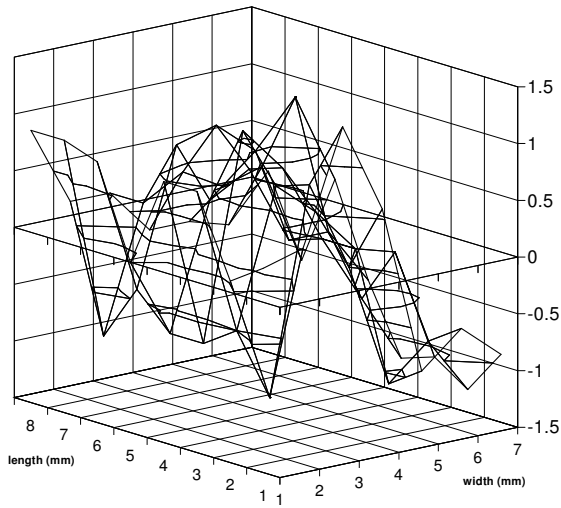


Fig. 9: Spatial responsivity uniformity of the AXUV100G photodiode at 121.6 nm.

Response uniformity at 240 nm of a 10 mm X 10 mm active area UVG photodiode is shown in Fig. 10 [16]. The response uniformity was within $\pm 0.5\%$ when scanned also with a 254 nm photon beam of 1 mm diameter. The excellent spatial response uniformity the UVG photodiodes will provide better reproducibility than other commercially manufactured photodiodes and therefore exhibit a lower overall measurement uncertainty.

Responsivity uniformity of 1 cm x 1 cm active area SXUV photodiodes (model # SXUV100) was found to be within $\pm 2\%$ when tested at 254, 162, 122 and 10 nm. Figure 11 shows a typical spatial responsivity uniformity plot for the SXUV100 photodiode at 121.6 nm when scanned with a 1 mm diameter beam.

Temperature Dependence:

Figure 12 shows the temperature dependence of the AXUV, SXUV and UVG diodes responsivity at 254 nm. Typically the responsivity was found to increase by .03% per degree Celsius. As shown in the center figure on back cover, the temperature dependence of AXUV and SXUV diode responsivity is essentially the same down to 1 nm. This suggests that the responsivity temperature dependence in this region is caused by an increase in the quantum yield (owing to reduction in the bandgap) with higher temperature [17].

Because of presence of surface recombination in the SXUV diodes, their responsivity temperature dependence is expected to be lower than that of the AXUV diodes. The surface recombination is known to have negative temperature dependence. However, we have not been able to verify the lower temperature dependence of the SXUV responsivity experimentally.

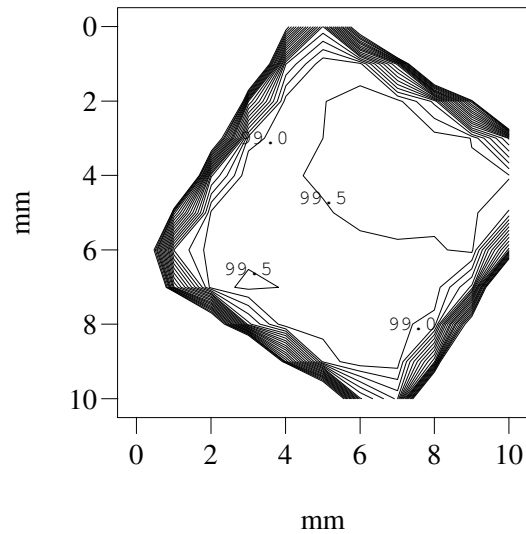


Fig. 10: Uniformity of IRD photodiode at 240 nm [15].

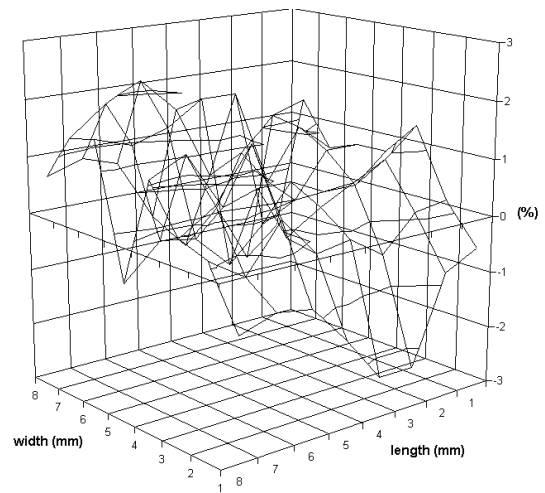


Fig. 11: Spatial responsivity uniformity of the SXUV100 photodiode at 121.6 nm

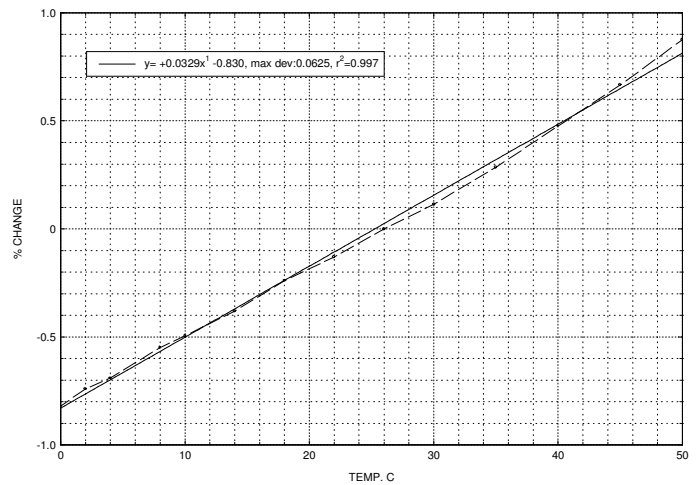


Fig. 12: Change in 254 nm responsivity of AXUV, SXUV and UVG photodiodes with temperature

AXUV/SXUV/UVG

Fig. 13 shows typical temperature dependence of the shunt resistance of AXUV/SXUV/UVG photodiodes. The shunt resistance was found to decrease by a factor of 2 for every 7 °C rise in temperature. This indicates that the dark current should double for every 7 °C rise in temperature.

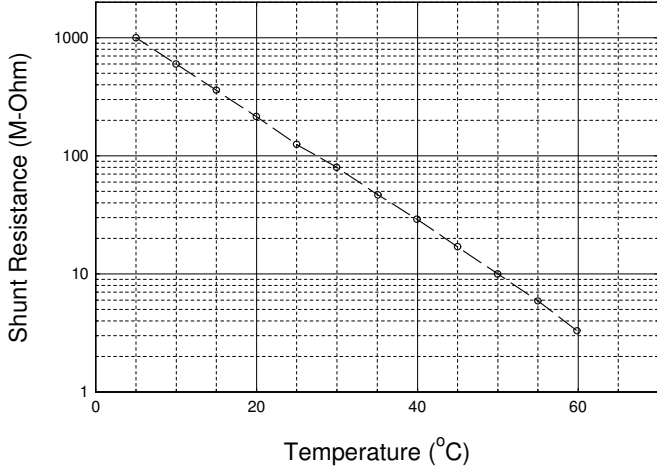


Fig. 13: Change in shunt resistance of AXUV, SXUV and UVG photodiodes with temperature.

Fig. 14 shows the typical temperature dependence of capacitance for the IRD photodiodes over a temperature range of 0°C to 40°C. The positive temperature dependence of diode capacitance occurs because the intrinsic carrier concentration increases with temperature which results in the reduction of built-in potential.

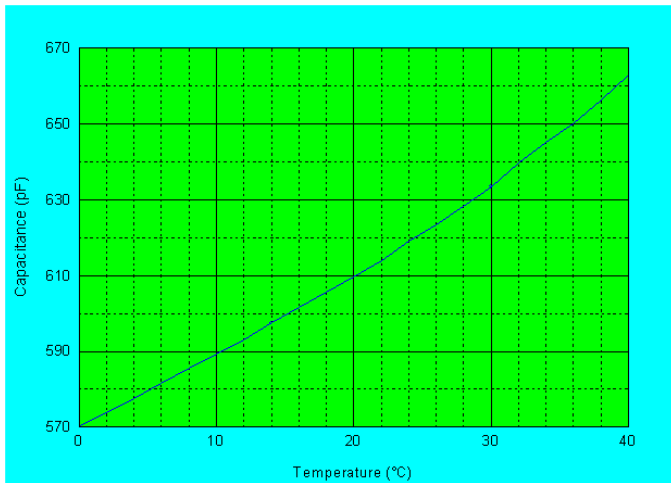


Fig. 14: Temperature dependence of zero bias capacitance of AXUV, SXUV and UVG diodes, with 5 mm dia active area.

Linearity/Dynamic Range:

Fig. 15 shows the linearity of the AXUV/SXUV/UVG photodiode and a widely used p-on-n photodiode of equivalent area when exposed to increasing levels of 430 nm CW radiation. All the diodes were tested without any reverse bias.

The standard ac-dc method was used to measure linearity. The p-on-n photodiode showed a noticeable decrease in responsivity at photocurrents greater than 500 μA while the IRD photodiodes showed only .02% decrease in responsivity at a photocurrent of 3 mA. Application of a reverse bias will extend the linear range of the photodiodes when measuring UV radiation. It is believed that the difference in the series resistance of these diodes can explain the large difference in linear range [7].

Response linearity to pulse radiation has been studied recently [6,18]. Higher the reverse bias on the detector, higher is the upper limit on the linear range. Because of their lower responsivity, SXUV diodes have higher upper limit of linear range compared with the AXUV and UVG diodes for a given reverse bias. Because of their high responsivity, IRD diodes can not be used for measurement of pulse energies in excess of 100 μJ even with a front attenuating layer or a directly deposited filter. For measurement of UV/EUV pulses with high energy, an attenuating metal mesh can be used in front of the diodes. Care needs to be taken to conduct the heat generated in the metal mesh which typically is in the vacuum system.

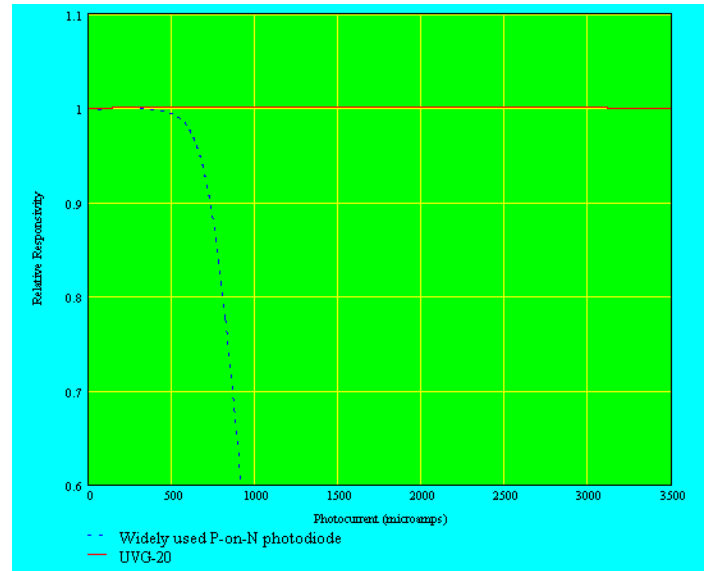


Fig. 15: Typical linearity of IRD photodiodes and a widely used P-on-N photodiode when tested at 430 nm.

Noise Characteristics:

Spontaneous fluctuations of current and voltage in electronic devices are called noise. When superimposed to a given signal, noise determines the lowest limit below which no signal can be reliably measured or amplified.

Thermal noise is the predominant noise source when IRD photodiodes are used without any external bias. When these are used with an external bias, shot noise will be the predominant noise source.

The thermal rms noise current, I_t is given by

$$I_t = (4kT\Delta f/R)^{1/2} \text{ [A]},$$

where K is the Boltzmann constant ($1.3807 \times 10^{-23} \text{ J K}^{-1}$), T is the absolute temperature [$^{\circ}\text{K}$], R is the shunt resistance [Ω], and Δf is the bandwidth of measurement [Hz]. For $1\text{ cm} \times 1\text{ cm}$ area diode with $1 \text{ G}\Omega$ shunt resistance at 22°C the noise current will be $4.1 \text{ fA (Hz)}^{-1/2}$.

In the literature the thermal noise is also called Nyquist noise and Johnson noise. When the diodes are used with external bias, the rms shot noise current, I_s , is given by

$$I_s = (2q\{I_d + I_{ph}\} \Delta f)^{1/2} \text{ [A]}$$

where q is the elemental electron charge, I_d is the dark current, I_{ph} is the photogenerated current and Δf is the bandwidth of the measuring equipment. Thus, for a dark current value of 10 nA and photogenerated current of 100 nA the shot noise current will be $1.876 \times 10^{-13} \text{ A/Hz}^{1/2}$.

Time Response:

The diode response time is determined by the resistance and capacitance present in the detector and measuring circuitry and the charge carrier transit time. Capacitance C of the diode is given by the silicon permittivity (ϵ), area (A), and the p-epitaxial layer thickness (D). For the AXUVHS5 diode with 25 micron silicon thickness the capacitance is:

$$C = \epsilon A/D = 10^{-12} \times (10^{-2}) / 25 \times 10^{-4} = 4 \text{ pF}$$

The diode series resistance is mainly governed by the distance electrons need to travel in the front field free n region towards the n^+ electrode. For small area diode like the AXUVHS5 this resistance is only a few ohms.

Using the 50Ω scope impedance, 5 ohm diode resistance and 4 pF capacitance the rise time (t_{RC}) given by $2.2 RC$ equals 0.48 ns . Worst case carrier transit time t_c , is a hole traveling across the entire depletion layer thickness. The time is given by the thickness (D) divided by the hole drift velocity. For the AXUVHS5 diode at 50 volt bias the electric field is $2 \times 10^4 \text{ V/cm}$ and the corresponding drift velocity is $5.3 \times 10^6 \text{ cm/sec}$ [19] giving rise to a transit time of 0.47 ns .

Adding the times in quadrature yields a theoretical rise time of 0.67 ns which is very close to the experimentally measured value of 0.7 ns .

It should be noted that carrier motion by diffusion process is completely neglected here which is a much slower process than the motion by drift. When a high speed photodiode like AXUVHS5 is fully exposed to radiation, carriers are also generated at the diode periphery. These carriers are collected by diffusion process because of absence of the electric field in this region. This results in the diode fall time much higher than the risetime. Therefore, to achieve almost equal rise and fall

times it is necessary that the radiation be limited only to the diode active area possibly using a pinhole.

Larger the diode area larger will be the distance electrons need to travel to the n^+ electrode. Therefore, large area diodes like AXUV20 have a series resistance around 20 Ohm . To reduce this resistance to 1 Ohm , AXUV20HS1 diodes have been specially fabricated which give 1 n-sec risetime when used with 150 volts bias (to reduce the drift time) and with a high speed amplifier (to get rid of 50 Ohm scope impedance).

Polarization Sensitivity:

The responsivity of silicon photodiodes can be affected by the degree of polarization and the azimuth of incident radiation. When a detector is used obliquely to incident radiation, polarization effects arise. The oxide thickness of the photodiode will affect the polarization sensitivity by means of surface reflectivity and absorption.

Polarization dependence of the diode responsivity has been reported in 50 nm to 150 nm spectral range [20]. This short wavelength polarization dependence implies that absorption in the oxide layer is the dominant loss mechanism (since there is little reflection loss) and it has been shown that absorption increases with larger angle of incidence due to increased path length. As oxide thickness is decreased, this polarization effect is reduced and at an oxide thickness of 8 nm (AXUV series diodes), this effect is negligible.

The AXUV photodiodes have been successfully used recently [21] to measure polarization of the EUV sources. A Mo/Si multilayer interference coating was deposited directly on the AXUV100 photodiode surface to selectively transmit the p-polarized component of 13.5 nm and to reflect the s-polarized incident radiation.

Polarization sensitivity of the SXUV diode responsivity between 130 and 600 nm is described in the literature [22].

Proper Use of the IRD Photodiodes [23]:

1) AXUV/UVG/SXUV series photodiodes can be used in air, in gas ambient like helium, argon, nitrogen, etc. and under vacuum lower than 10^{-10} torr . Devices with suffix EUT need to be selected for extremely low level vacuum applications like 10^{-10} torr . IRD photodiodes can be vacuum baked up to 200°C . They can be operated in the temperature range of -200°C to 70°C .

2) It is advisable to check the photodiode for functionality before placing it into the location of measurement such as a vacuum chamber. Do this by connecting the leads of the diode to the positive and negative terminals of a picoammeter or electrometer and exposing the diode to room light. As an example, an uncoated $1 \text{ cm} \times 1 \text{ cm}$ photodiode should produce an output current of 20 to $200 \text{ micro amperes}$ depending on room light intensity. A filtered photodiode should have an output current of less than a few nano-amperes. A table lamp

or flashlight can also be used to check the filtered diode functionality if room light conditions do not produce a measurable output.

3) To avoid contribution of the photo emission current to the photogenerated current, the signal should be read from the p-region (anode) of the diode with n-region (cathode) grounded. A significant photo emission current contribution has been noticed in the AXUV diodes in 70 nm to 140 nm region when the signal is read from the n-region with p-region grounded.

4) Condensables within the vacuum system in which IRD photodiodes are used must be maintained at as low a level as possible. A surface film deposited on the diode will absorb radiation and may even fluoresce. In either of these cases, a permanent film could result from interaction with XUV radiation leading to irreversible changes in device efficiencies.

5) As the most of the IRD photodiodes are windowless devices, precaution should be taken not to breathe, sneeze or touch the active area of the devices. If by accident the active area is contaminated, the surface can be cleaned by an acetone or alcohol dipped swab. As the IRD diodes have very shallow junction, the swabbing action should be gentle without any pressure. All the filtered diodes with carbon and silicon passivating coating (for example AXUV100 Mo/Si, AXUV100 Ti/C etc.) can also be cleaned by the above method. Please contact IRD for instructions on cleaning photodiodes with other directly deposited filters.

6) Care must be taken to avoid disturbing the delicate wire bonds which connect the photodiode chip to the package pins. If the wire becomes pushed down against the chip, a short will result. If this happens, use a fine wire or needle to gently lift the wire bond away from the chip surface (a microscope will usually be needed). If the wire bonds are broken the device can be sent back to IRD for repair. Most of the IRD photodiodes are assembled with multiple bonds and in most cases, redundant pins. Only one wire bond per pin is necessary for proper operation of the device.

7) Most of the AXUV/UVG/SXUV diodes can be purchased with protective epoxy on their wire bonds so that the bonds will not break if touched accidentally. However, the diodes whose wire bonds are protected by epoxy need to be operated near room temperature, i.e., one can not heat these devices for out gassing purpose nor cool them to reduce the noise. This is necessary to avoid generation of stress on the wires because of difference in the Thermal Coefficient of Expansion (TCE) between the wire and the epoxy.

8) Linear range of AXUV/UVG/SXUV diodes can be increased several times by application of a small reverse bias. Thus, under high level radiation condition, the diode saturation can easily be checked by application of one to two volts reverse bias. In extreme cases, in excess of one hundred volts reverse bias is applied to the diodes to operate them in the linear range. A simple series circuit of the voltage source, diode and current measuring device is required when the

source is a CW source. Make sure the diode is reverse biased and not forward biased as this may damage the diode. When using the diodes for pulse energy measurements usually an external bias T, like BT250 is required.

9) Care should be used while using the small active area diodes like the AXUVHS5 as absolute devices. All the AXUV products can be used as absolute devices provided that radiation beam is limited to the diode active area. When the diode is flooded (overfilled) with the beam, it is hitting the diode periphery, the quantum efficiency of which is not known. Detectors with active area as large as 24mm x 24mm are available from IRD to make absolute intensity measurement of large beams.

10) Since photodiodes are subject to damage by excessive heat, care must be given to soldering temperature and dwell time. As a guide, metal package devices should be soldered at a maximum of 260 °C within 10 seconds and ceramic package devices at 260 °C within 5 seconds at 2 mm minimum distance from package base. Use acetone or alcohol to remove solder flux. To avoid contamination of the active area, the protective window shipped with the photodiode should be left on during soldering.

High Energy X-Rays:

AXUV standard photodiodes have an effective silicon thickness of 10 to 104.6 microns for n-on-p photodiodes. Thus, a fraction of photons with energies above 4000 eV will transmit through the active silicon reducing their quantum efficiency from the designed 100% value. As this reduction is solely caused by the limited silicon thickness, the AXUV diodes can also be used as absolute x-ray devices if silicon thickness is known. AXUV100 photodiodes (10mm x 10mm active area) with measured silicon thickness up to 105 microns with a measurement uncertainty of $\pm 5\%$ are available as standard products. The AXUV-20HE1 photodiodes have a silicon thickness of 425 microns and will have 100 % collection of photons up to 10 keV. However, because of high noise in these devices, use of the AXUV100 devices with known silicon thickness is recommended. Photodiodes with custom thicknesses can also be manufactured. AXUVPN100 diodes, which are p-on-n photodiodes, have

Theoretical responsivity, S , as a function of x-ray energy may be obtained once the absorption $A(\epsilon_{ph})$ of the silicon layer is known. The absorption may be obtained from public sources such as LBL for photon energies up to 30 keV [24] and NIST for photon energies above 30 keV [25]. Once the absorption is known, the following formula may be used to calculate the responsivity

$$S(\epsilon_{ph}) = Q(\epsilon_{ph})/\epsilon_{ph} = F_f A(\epsilon_{ph})/3.66 (A/W)$$

The value of 3.66 is an average value for electron-hole pair creation energy (eV) in silicon. The factor F_f is a fluorescence factor taken as 0.95 to account for about 5% x-ray fluorescence yield in silicon for photons with energy larger than 1838 eV.

Silicon fluorescence yield has been experimentally measured for photons with energy up to 9 keV [26]. It may be possible that some of the silicon fluorescence gets reabsorbed for higher energy photons leading to a higher responsivity than that calculated by the above equation. NIST values include fluorescence and fluorescent light reabsorption in their calculations.

Figure 16 shows calculated responsivity for 45, 100 and 425 μm thick silicon. Figure 17 shows a comparison of responsivity calibrated at PTB and calculated using NIST and LBL data using 105 μm silicon thickness.

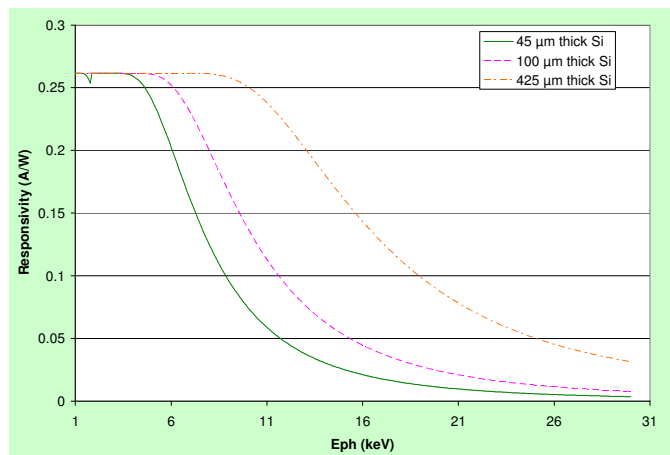


Fig. 16: Responsivity of AXUV photodiodes with 45, 100 and 425 micron effective Si thicknesses.

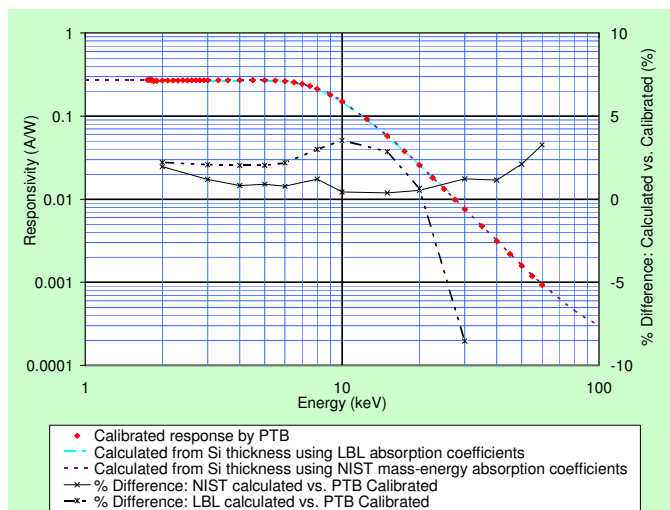


Fig. 17: Responsivity calculated using both NIST and LBL transmission values, 53 μm effective Si thicknesses.

Applications:

The AXUV photodiodes have several advantages over the orthodox tube-type XUV detectors. The AXUV photodiodes exhibit very low noise, do not need external voltages for their operation, are insensitive to magnetic fields, cost less to fabricate, have low mass and have large collection area to size ratio making them extremely attractive for use in satellites and deep space probes.

These diodes have been approved as transfer standards in the XUV spectral range because of their ease of use, excellent stability and spatial homogeneity of quantum efficiency, large dynamic range (over eight orders of magnitude), small size, ruggedness, and ultrahigh vacuum compatibility. These diodes are operated in the open face configuration down to Angstrom wavelengths, even in the presence of gases. This feature gives the AXUV diode based spectrometers an important advantage over present XUV spectrometers based on conventional detectors, which need to be used either in vacuum or with a window.

Due to these unique features, AXUV photodiodes have been successfully used in the European SOHO and Coronas-Photon, and American SNOE, SORCE, GOES, TIMED and EOS solar space instrumentation.

An AXUV multi-element diode array has been successfully used in a Ring Accelerator Experiment (RACE) at Lawrence Livermore National Laboratory and also by other fusion research laboratories around the world to obtain radiated power vs. length and radius profiles of the plasma. Owing to its fast response speed, the array was found to yield excellent time resolution of power in quasisteady plasma transients.

A four channel compact neutral particle analyzer using AXUVHS5 photodiodes was used recently to observe 50 to 350 keV hydrogen neutrals [27].

Small active area AXUV diodes optimized for high response speed were found to be ideal detectors for XUV measurements in a joint US/Russian magnetized target fusion experiment. The performance of the AXUV diodes tested was found to be comparable with that of diamond detectors with orders of magnitude lower cost.

Several quadrant AXUV diodes with central holes and rectangular slit openings have been built specifically for synchrotron beam intensity monitoring and position sensing. Because of its 5 micron physical silicon thickness, the AXUV36 diode can be used in transmission mode for continuous intensity monitoring of the x-ray beam. These devices have proven to be very useful since the unstable nature of synchrotron radiation beam is an important source of experimental error.

Radiometric Characterization:

Because of its unique test facilities, IRD provides services for radiometric characterization of semiconductor photodiodes in 200 nm to 2600 nm spectral region. Spectral responsivity, reflectance and internal quantum efficiency, their temperature dependence, response uniformity and the dynamic range are routinely measured at IRD.

A fully automated Optronic Labs 750-M-D double monochromator is used to measure the responsivity, reflectance and their temperature dependence. Photodiode uniformity is measured by scanning a 1 mm diameter light

beam with a computer controlled x-y stage. Standard ac/dc method is used to determine the diode linear range.

Stability tests for the photodiodes are measured at facilities at NIST, LBL, and PTB. These facilities routinely provide fluences of 10^{22} photons/cm² at 100 eV for stability testing of the IRD photodiodes.

References:

- 1] R. Korde and J. Geist, "Quantum Efficiency Stability of Silicon Photodiodes", *Applied Optics*, Vol. 26, 5284-5290 (1987).
- 2] L.R. Canfield et. al. "Absolute Silicon Photodiodes for 160 nm to 254 nm Photons", *Metrologia*, Vol. 35, 329-334 (1998).
- 3] H.O. Funsten et. al. "Response of 100% Internal Quantum Efficiency Silicon Photodiodes to 200 eV to 40 keV Electrons", *IEEE Transactions on Nuclear Science*, Vol. 44, No. 6, 2561-2565 (1997).
- 4] H.O. Funsten et al. "Response of 100% Internal Carrier Collection Efficiency Silicon Photodiodes to Low-Energy Ions", *IEEE Transactions on Nuclear Science*, Vol.48, No 6, 1785-1789 (2001).
- 5] C.S. Silver et. al. "Silicon photodiodes for low-voltage electron detection in scanning electron microscopy and electron beam lithography", *J. Vac. Sci. Technol.*, Vol 24, No. 6, 2951-2955 (2006)
- 6] R. Stuik and F. Bijkerk "Linearity of P-N junction photodiodes under pulsed irradiation", *Nuclear Instruments and Methods in Physics Research A* 489, 370-378 (2002).
- 7] R. Korde et. al. "Present Status of Radiometric Quality Silicon Photodiodes", *Metrologia*, Vol. 40, S145-S149 (2003).
- 8] R. Korde, J. Cable and R. Canfield, "100% Internal Quantum Efficiency Silicon Photodiodes with One G-rad Passivating Silicon Dioxide" *IEEE Trans. on Nuclear Sciences*, Vol. 40, No. 6, 1655-1659 (1993).
- 9] F. Scholze, H. Rabus, G. Ulm "Spectral responsivity of silicon photodiodes: High-accuracy measurement and improved self calibration in the soft X-ray spectral range" *Proc. SPIE* 2808, 534-543 (1996).
- 10] R. Korde et. al. "The effect of Neutron Irradiation on Silicon Photodiodes" *IEEE Trans. on Nuclear Sciences*, Vol. 36, 2169-2175 (1989).
- 11] T. English et. al. "Neutron Hardness of Photodiodes for use in Passive Rubidium Standards", *Proc. Of the 42nd Annual Frequency Control Symposium*, IEEE, 532-539 (1988).
- 12] C. Jorquera et. al. "Design of New Photodiode Standards for use in the MISR In-Flight Calibrator" *Proc. of IGARSS'94*, IEEE Catalog Number 94CH3378-7, 1998-2000 (1994).
- 13] See also : K. Solt et. al. "PtSi-n-Si Schottky-barrier Photodetectors with Stable Spectral Responsivity in the 120-250 nm Spectral Region", *Appl. Phys. Lett.*, Vol. 69 3662-3664 (1996).
- 14] F. Scholze et. al. "Irradiation Stability of Silicon Photodiodes for Extreme-ultraviolet Radiation", *Applied Optics*, Vol. 42, No. 28, 5621-5626 (2003).
- 15] K. Shenai. "Manufacturability Issues Related to Transient Thermal Annealing of Titanium Silicide Films in a Rapid Thermal Processor", *IEEE Transactions on Semiconductor Manufacturing*, Vol. 4, 1-8 (1991).
- 16] Ping-Shine Shaw et. al. "The new ultraviolet spectral responsivity scale based on cryogenic radiometry at Synchrotron Ultraviolet Radiation Facility III", *Rev. of Sci. Instruments*, Vol. 72, 2242-2247 (2001).
- 17] B. Kjornrattanawanich et. al. "Temperature Dependence of the EUV Responsivity of Silicon Photodiode Detectors". *IEEE Transactions on Electron Devices*, Vol. 53, 218-223 (2006).
- 18] R.E. Vest and Steven Grantham "Response of a Silicon Photodiode to Pulsed Radiation", *Applied Optics*, Vol. 42, No. 25, 5054-5063 (2003).
- 19] For example, see: quick reference manual for silicon integrated circuit technology by W.E. Beadle et. al. John Wiley and Sons (1985).
- 20] T. Saito and H. Onuki "Difference in Silicon Photodiode Response Between Collimated and Divergent Beams", *Metrologia*, Vol. 37, 493-496 (2000).
- 21] B. Kjornrattanawanich et. al. "Temperature and Polarization Performance of EUV Silicon Photodiodes", Paper presented at the Eighth International Conference on Synchrotron Radiation Instrumentation, San Francisco, (2003).
- 22] Ping-Shine Shaw et. al. "Characterization of an UV and VUV Irradiance Meter with Synchrotron Radiation", *Applied Optics*, Vol. 41, No. 34, 7173 (2002)
- 23] See also: "Photodiode Detectors" by L.R. Canfield in "Vacuum Ultraviolet Spectroscopy II", Eds. J.A. Sampson and D.L. Ederer, Academic Press, (1998).
- 24] Center for X-ray Optics, Lawrence Berkeley Laboratory http://www-cxro.lbl.gov/optical_constants/
- 25] Physical Laboratory Physical Reference Data, National Institute of Science and Technology <http://physics.nist.gov/PhysRefData/XrayMassCoef/cover.html>
- 26] J.L. Campbell et. al. "Experimental K-shell fluorescence yield of silicon" *J. Phys. B: At. Mol. Opt Phys.*, Vol. 31, 4765-4779 (1998).
- 27] V. Tang et al. "Compact multichannel neutral particle analyzer for measurement of energetic charge-exchanged neutrals in Alcator C-mod" *Review of Scientific Instruments*, Vol 77, 083501-1 – 8, (2006).

Diodes with Integrated Bandpass Filters

To avoid use of fragile freestanding thin film filters during XUV experiments and also in space missions, visible blind AXUV and SXUV photodiodes with integrated thin film filters have been developed. The following table lists available AXUV and SXUV diodes with different filter materials and their passbands. Typical visible light transmission of these filtered diodes is less than 10^{-4} . Diodes with higher visible light blocking can be specially selected if required. IRD is continuously making diodes with many different filters. Users are requested to contact us for their special filter requirements.

The advantages of these integrated detector-filter devices over presently used separate freestanding thin foil filters and detectors are compactness, higher reliability, ease in manufacturing and handling, more stable bandpass and

flexibility in design as the filter thicknesses are determined by optical constants and not by the mechanical strength requirement.

Owing to these advantages filtered AXUV diodes have been successfully used in several rocket experiments and satellites to measure the solar EUV radiation. The SXUV filtered diodes are being used to characterize the EUV lithography sources and also are being used in the EUV steppers.

We anticipate that the filtered diodes will be extremely useful in future space missions and other applications like soft x-ray radiometry, x-ray and EUV lithography, x-ray microscopy and XUV spectroscopy and plasma diagnostics.

PRODUCT NAME	FILTER THICKNESS (nm)	PASS BAND (nm)	PRODUCT NAME	FILTER THICKNESS (nm)	PASS BAND (nm)
AXUV100Cr/W/Au	8/100/400	< 1	AXUV100In/SiC	200/20	76-105
AXUV100Al/Fe	400/450	1.7-3.5	AXUV100LA	200	117-131
AXUV100Al/Mn2	500/500	1.9-3.5	AXUVSP2Al	150	17-80
AXUV100Al/V	400/600	2.4-3.5	AXUV96Ti/Mo/C	70/200/50	5-13
AXUV100Ti/Zr/Al	250/100/100	2.8-5	AXUV96Al	300	17-80
AXUV100Al/CaF ₂ /Ag	200/1000/250	3.6-5.2	AXUV96Sn	200	53-74
AXUV100Ti/Mo/Au	40/200/100	5-12	AXUV96In/SiC	200/10	76-105
AXUV100Ti/Mo/C	50/200/70	5-13	AXUV20Ti/Mo/C	70/200/50	5-13
AXUV100Ti/Mo/Si/C	40/200/100/50	5-15	AXUV20Zr/C	200/50	6-16
AXUV100Zr/C	200/50	6-16	AXUV20Si/Zr	100/200	11-18
AXUV100Ti/Zr/Au	20/200/100	6-12	AXUV20Mo/Si	350/500	12.2-15.8
AXUV100Ti/C	500/50	<7	AXUV20Al	300	17-80
AXUV100Ti/Pd	200/100	<11	AXUV20Ti/C	200/50	<7
AXUV100Si/Zr	100/200	11-18	AXUV20HS1Si/Zr	100/200	11-18
AXUV100Mo/Si	350/500	12.2-15.8	AXUV20HS1Mo/Si	350/500	12.2-15.8
AXUV100Ti/C2	200/50	< 12	AXUV20HS1Al5	300	17-18
AXUV100Al/Zr	125/125	17-21	AXUV20ASi/Zr	100/200	11-18
AXUV100Al	150	17-80	AXUVHS5Si/Zr	100/200	11-18
AXUV100Al2	40	17-80	AXUV20AMo/Si	350/500	12.2-15.8
AXUV100GA12	50	17-80	AXUV20BNC-Si/Zr	100/200	11-18
AXUV100Al3	100	17-80	SXUV100Mo/Si/SiC	250/200/50	11-16
AXUV100Al4	1000	17-80	SXUV100Si/Zr	100/200	11-18
AXUV100Al5	300	17-80	SXUV100Mo/Si	350/500	12.2-15.8
AXUV100Al/C	200/50	17-36	SXUV20HS1Si/Zr	100/200	11-18
AXUV100Al/Nb/C	250/50/50	17-21	SXUV20HS1Mo/Si	350/500	12.2-15.8
AXUV100Al/Mn3	270/100	25-40	SXUV20HS1Mo/Si/SiC	500/500/50	12.5-14.5
AXUV100Al/Mn	200/100	25-40	SXUV20AMo/Si	350/500	12.2-15.8
AXUV100Cr/Al	60/150	27-40	SXUVHS5Mo/Si	350/500	12.2-15.8
AXUV100Cr/Al3	100/270	27-37	SXUVHS5Si/Zr	50/480	11-18
AXUV100Cr/Al2	100/200	27-37	SXUV300C-Mo/Si/SiC	500/500/50	12.5-14.5
AXUV100Sn (2% Ge)	200/10	53-74	SXUV20AMo/Si/SiC	250/200/50	11-16

Ref. N.E. Lanier et. al. "Low-cost, robust, filtered spectrometer for absolute intensity measurements in the soft x-ray region", Review of Scientific Instruments, Vol 72, No. 1, 1188-1191 (2001).

AXUV Absolute Devices/Transfer Standards

Model no.	Sensitive Area (mm ²)	Size (mm)	Shunt Resistance (MΩ)**	Capacitance @ 0V (nF)**	Risetime (10-90%) (μSec)**	Package/ Page no.
AXUV100	100	10 X 10	100	20	10	C100/17
AXUV100GX	100	10 X 10	100	20	10	C100GX/23
AXUV100PC	100	10 X 10	100	20	10	PC100/23
AXUV100TSA-Flange	100	10 X 10	100	20	10	C100F/24
AXUVPN100	100	10 X 10	100	4	10	C100PN/25
AXUV96	96	6 X 16	100	20	10	M96/17
AXUVSP2	96	6 X 16	100	20	10	CSP2/17
AXUV20	20	5 Ø	1000	4	2	TO8A/17
AXUV20A	24	5.5 Ø	1000	4	2	C20/17
AXUV20BNC	20	5 Ø	1000	4	2	BNC/17
AXUV20HE1 [®]	20	5 Ø	10	0.5	1	C20HE/17
AXUV50HE1 [®]	50	8 Ø	10	3	6	C50HE/17
AXUV12#	12	4 Ø	1000	2	1	TO5A/20
AXUV10	10	10 X 1	1000	2	2	C10/17
AXUV300	330	22 X 15	40	40	15	P300/18
AXUV300C	330	22 X 15	40	40	15	C300/18
AXUV300M/G	330	22 X 15	40	40	15	M300/18
AXUV576	576	24 X 24	20	1000	500	M576/18
AXUV576C-EUT	576	24 X 24	20	80	25	C576/18
AXUV2300	2304	24 X 24 (X4)	5	200	25	C2300/24
AXUV36*	36	6 X 6	10	10	10	M36/20

Ref: 1) "Stable silicon photodiodes for absolute intensity measurements in the VUV and soft x-ray regions" E.M. Gullikson et.al., J. of Electron Spectroscopy and Related Phenomena, Vol. 80, 313-316 (1996)

2) "Fundamental limits to detection of low-energy ions using silicon solid-state detectors" Funsten et.al., Applied Physics, Vol. 84, no. 18, 3552-3554 (2004)

AXUV High speed

Model no.	Sensitive Area (mm ²)	Size (mm)	Dark Current @ 50V	Capacitance @ 0V (pF)	Risetime (10-90%) (pSec)	Package/ Page no.
AXUV5 [†]	5	2.5 Ø	10 nA	500	2000	TO5B/20
AXUV20HS1 [†]	20	5 Ø	50 nA	700	1000	C20/17
AXUV20HS1BNC [†]	20	5 Ø	50nA	700	1000	BNC/17
AXUV63HS1 [†]	63	9 Ø	20 nA	2000	2000	C63/20
AXUV63HS1-CH/LP [†]	63	9 Ø	20 nA	2000	2000	M63LP/20
AXUVHS1#	0.05	0.22 X 0.22	100 pA	5	250	SMA/21
AXUVHS2#	0.05	0.22 X 0.22	100 pA	5	250	SSMA/21
AXUVHS3#	0.005	0.07 X 0.07	50 pA	2	80	SSMA/21
AXUVHS4#	0.026	0.16 X 0.16	100 pA	10	200	SMA/21
AXUVHS5#	1	1 X 1	200 pA	40	700	SMA/21
AXUVHS5A#	1	1 X 1	200pA	40	700	TO46/20
AXUVHS6#	0.00063	0.025 X 0.025	20 pA	1	50	SSMA/21
AXUVHS11 [†]	0.28	0.6 Ø	200 pA	10	250	SMA/21

Ref: 1) "Silicon photodiode characterization from 1 eV to 10 keV" G.C. Idzorek and R.J. Bartlett, SPIE, Vol. 3114, 349-356 (1997)

** Devices with better values may be selected, at no additional cost.

@ 100% quantum efficiency for up to 10 KeV photons.

* With 5 micron physical thickness

Use with 50 volts bias.

† Use with 150 volts bias.

AXUV Arrays

Model no.	Sensitive Area (mm ²)	Size (mm)	Shunt Resistance (MΩ)**	Capacitance @ 0V (pF)**	Risetime (10-90%) (nSec)**	Package/ Page no.
AXUV3ELA#	1 (X3)	1 X 1 (X3)	1000	40	1	C3EL/21
AXUV10EL#	1 (X10)	1 X 1 (X10)	1000	40	1	C10EL/21
AXUV16ELO/G	10 (X16)	2 X 5 (X16)	100	2000	500	C16ELO/21
AXUV16EL	10 (X16)	2 X 5 (X16)	100	2000	500	C16EL/22
AXUV20EL	3 (X20)	0.75 X 4 (X20)	300	1000	200	C20EL/22
AXUV22EL	4 (X22)	1.0 X 4.0 (X20)	200	1000	200	C22EL/22
AXUV42EL	10.2 (X42)	1.1 X 9.6 (42)	10	2000	500	M42EL/24
AXUV3CR	EL 1: 36.3 EL 2: 19.8 EL 3: 4.2	EL 1: 5.9 – 9.2 EL 2: 2.7 – 5.7 EL 3: .74 – 2.5	20	EL 1: 700 EL 2: 350 EL 3: 81	100	M3CR/23

- Ref: 1) "High resolution bolometry on the Alcator C-Mod tokamak (invited)" R.L. Boivin et.al., Rev. of Sci. Instrum Vol. 70 (1), 260-264 (1999)
 2) "Fast bolometric measurements on the TCV Tokamak" I. Furno et.al. Rev. of Sci. Instrum. Vol. 70 (12), 4552-4556 (1996)
 3) "Time resolved radiated power during tokamak disruptions and spectral averaging of AXUV photodiode response in DIII-D" D.S. Gray et.al., Rev. of Sci. Instrum., Vol. 75, no. 2, 376-381 (2004)

AXUV Position Sensing

Model no.	Central Slit (mm)	Sensitive Area (mm ²)	Size (mm)	Shunt Resistance (MΩ)**	Capacitance @ 0V (nF)**	Risetime (10-90%) (μSec)**	Package/ Page no.
AXUVPS1†	0.5 Ø	11 (X4)	7.6 Ø	100	2	2	PS1/18
AXUVPS1A†	0.7 Ø	11 (X4)					
AXUVPS1B†	1 Ø	10.75 (X4)					
AXUVPS1D†	.5 X 2.5	10.75 (X4)					
AXUVPS1E†	2 X 4	9 (X4)	7.6 Ø	100	2	2	MTO8/19
AXUVPS1F†	5 Ø	6 (X4)					
AXUVPS1G†	1.6 Ø	10.5 (X4)					
AXUVPS6†	N/A	11 (X4)					
AXUVPS2	1 X 2	24.5 (X4)	5 X 5	100	5	4	PS2/19
AXUVPS2/LP	1 X 2	24.5 (X4)	(X4)				PS2LP/20
AXUVPS3	N/A	25 (X4)	5 X 5	100	5	4	PS2/19
AXUVPS3C			(X4)				PS3C/19
AXUVPS4	N/A	1.25 (X4)	2.5 Ø	1000	0.18	0.1	PS4/19
AXUVPS4C							PS4C/19
AXUVPS5	N/A	24 (X4)	3 X 8	100	5	4	PS5/18
AXUVPS7	5.6 Ø	38 (X4)	15 Ø	10	1.2	2	PS7/23
AXUVPSV	*	315	15X21	10	40	15	PSV/18
AXUV600M	N/A	150 (X4)	27 X 27	20	30	12	M600/18

- Ref: 1) "A beam tracking optical table for synchrotron x-ray beamlines" R.G. Van Silfhout, NIMS,A,Vol. 403, 153-160 (1998)
 2) "Feasibility study into the use of silicon photo-diodes for the alignment of collimated X-rays on the SRS" S.G. Buffey, NIMS, A, Vol. 431, 334-337 (1999)

Use with 50 volts bias.

* Four detectors are needed to realize a variable x-y slit.

** Devices with better values may be selected, at no additional cost.

† Available in low profile packages, see the PS1LP package, page 19.

SXUV Products

Model no.	Sensitive Area (mm ²)	Size (mm)	Shunt Resistance (MΩ)**	Capacitance @ 0V (nF)**	Risetime (10-90%) (μSec)**	Package/ Page no.
SXUV100	100	10 X 10	20	15	6	C100/17
SXUV100RPD	100	10 X 10	20	15	6	C100/17
SXUV20RPD	20	5.0 Ø	100	4	2	TO8A/17
SXUV20A	24	5.5 Ø	100	4	2	C20/17
SXUV20BNC	20	5.0 Ø	100	4	2	BNC/17
SXUV20C	24	5.5 Ø	100	4	2	TO8C/17
SXUV576C	576	24 X 24	5	80	50	C576/18
SXUV300	330	22 X 15	10	40	15	M300/18
SXUV300C	330	22 X 15	5	40	15	C300/18
SXUV10A	10	1X10	400	1	0.6	C10A/17
SXUV5	5	2.5 Ø	200	1	0.5	TO5B/20
SXUV5S	5	2.5 Ø	200	1	0.5	TO5S/20
SXUV100mj [§]	100	10 X 10	20	15	6	100mj/22

SXUV Position Sensing

Model no.	Central Slit (mm)	Sensitive Area (mm ²)	Size (mm)	Shunt Resistance (MΩ)	Capacitance @ 0V (nF)**	Risetime (10-90%) (μSec)**	Package/ Page no.
SXUVPS1†	0.5 Ø	11 (X4)	7.6 Ø	10	2	2	PS1/18
SXUVPS1/LP	0.5 Ø	11 (X4)	7.6 Ø	10	2	2	PS1LP/19
SXUVPS1A†	0.7 Ø	11 (X4)	7.6 Ø	10	2	2	MTO8/19
SXUVPS1B†	1.0 Ø	10.75 (X4)					
SXUVPS1D†	.5 X 2.5	10.75 (X4)					
SXUVPS1E†	2 X 4	9 (X4)					
SXUVPS1F†	5 Ø	6 (X4)					
SXUVPS1G†	1.6 Ø	10.5 (X4)					
SXUVPS6	N/A	11 (X4)	7.6 Ø	10	2	2	MTO8S/19
SXUVPS6S	N/A						
SXUVPS2	1 X 2	24.5 (X4)	5 X 5	10	5	4	PS2/19
SXUVPS2/LP	1 X 2	24.5 (X4)	(X4)				PS2LP/20
SXUVPS3	N/A	25 (X4)	5 X 5	10	5	4	PS2/19
SXUVPS3C	N/A		(X4)				PS3C/19
SXUVPS4C	N/A	1.25 (X4)	2.5 Ø	200	0.18	0.1	PS4C/19
SXUVPS4S	N/A	1.25 (X4)	2.5 Ø	200	0.18	0.1	PS4S/19
SXUVPS5	N/A	24 (X4)	3 X 8	20	5	12	PS5/18
SXUV600M	N/A	150 (X4)	27X27	5	30	15	M600/18

** Devices with better values may be selected, at no additional cost.

† Available in low profile packages, see the PS1LP package, page 19

§ For mJ pulse detection

SXUV High Speed

Model no.	Sensitive Area (mm ²)	Size (mm)	Shunt Resistance (MΩ)**	Capacitance @ 0V (nF)**	Risetime (10-90%) (μSec)**	Package/ Page no.	Model no.
SXUVHS5#	1	1 X 1	200	1 nA	40	700	SMA/21
SXUVHS5A/HS5S#	1	1 X 1	200	1 nA	40	700	TO46/TO46S/20
SXUVHS5FILTER#	1	1 X 1	100	2 nA	40	700	CHS5/21
SXUV20HS1†	20	5 Ø	100	20 nA	950	1000	C20/17
SXUV20HS1BNC†	20	5 Ø	100	20 nA	950	1000	BNC/17

UVG Absolute Devices/Transfer Standards

Model no.	Sensitive Area (mm ²)	Size (mm)	Shunt Resistance (MΩ)**	Capacitance @ 0V (nF)**	Risetime (10-90%) (μSec)**	Package/ Page no.
UVG100	100	10 X 10	100	20	10	C100/17
UVG300	330	22 X 15	20	40	15	P300/18
UVG576	576	24 X 24	10	100	50	M576/18
UVG20	20	5 Ø	1000	4	2	TO8A/17
UVG20BNC	20	5 Ø	1000	4	2	BNC/17
UVG20B	24	5.5 Ø	1000	4	2	C20/17
UVG20C	24	5.5 Ø	1000	4	2	TO8C/17
UVG12	12	4 Ø	1000	2	1	TO5A/20

UVG High Speed

Model no.	Sensitive Area (mm ²)	Size (mm)	Shunt Resistance (MΩ)	Dark Current @ 50V	Capacitance @ 0V (pF)	Risetime (10-90%) (nSec)	Package/ Page no.
UVG5†	5	2.5 Ø	1000	2 nA	200	< 2	TO5B/20
UVG5SI†	5	2.5 Ø	1000	2 nA	200	< 2	TO5SI/23
UVGHS1#	0.05	0.22 X 0.22	1000	100 pA	5	0.25	SMA/21
UVGHS2#	0.05	0.22 X 0.22	1000	100 pA	5	0.25	SSMA/21
UVGHS3#	0.005	0.07 X 0.07	1000	50 pA	2	0.08	SSMA/21
UVGHS4#	0.026	0.16 X 0.16	1000	100 pA	10	0.2	SMA/21
UVGHS5#	1	1 X 1	1000	200 pA	40	0.7	SMA/21
UVGHS6#	0.00063	0.025 X 0.025	1000	20 pA	1	0.05	SSMA/21

UVG Other Products

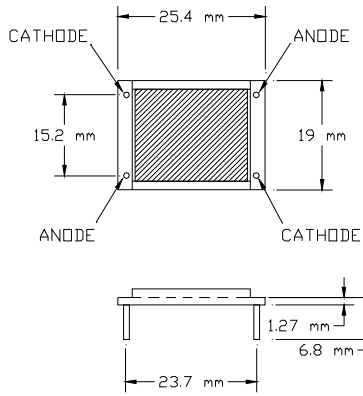
Model no.	Sensitive Area (mm ²)	Size (mm)	Shunt Resistance (MΩ)**	Capacitance @ 0V**	Risetime (10-90%)	Package/ Page no.
UVG100S	100	10 X 10	100	20 nF	10 μsec	C100S/22
UVG20S	24	5.5 Ø	1000	4 nF	2 μsec	C20S/22
UVG10	10	10 X 1	1000	2 nF	1 μSec	C10/17
UVG5S	5	2.5 Ø	1000	1 nF	0.5 μSec	TO5S/20

#Use with 50 V bias

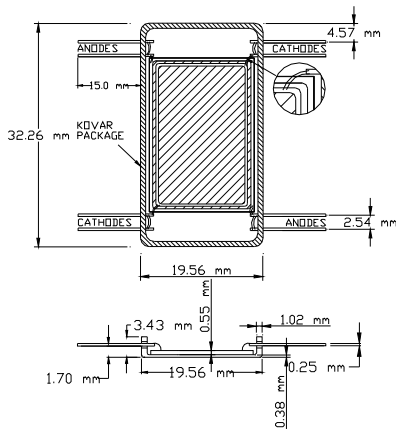
** Devices with better values may be selected, at no additional cost.

†Use with 150 V bias

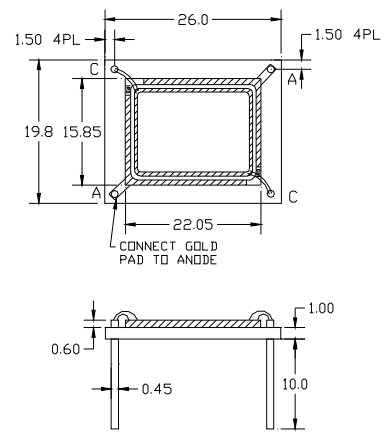
Note: All the UVG series devices without front window are shipped with epoxy on the wirebonds, unless requested otherwise.



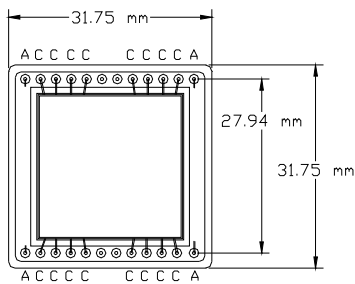
P300



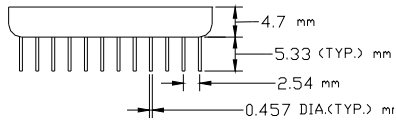
M300



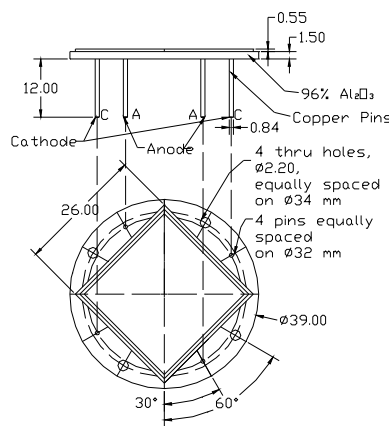
C300



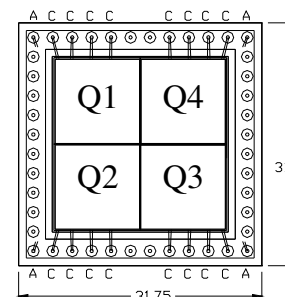
A - ANODES
C - CATHODES



M576

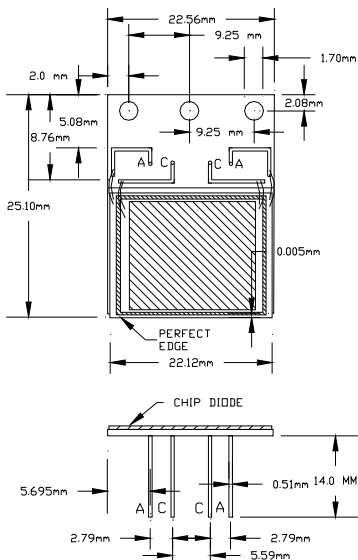


C576

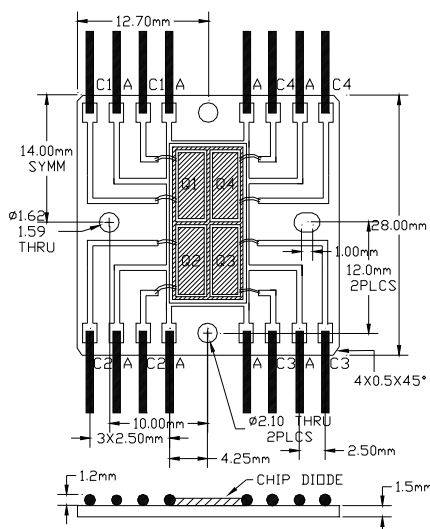


C - Cathode
A - Anode

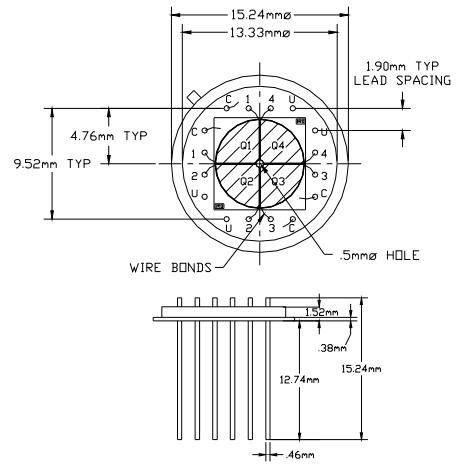
M600



PSV



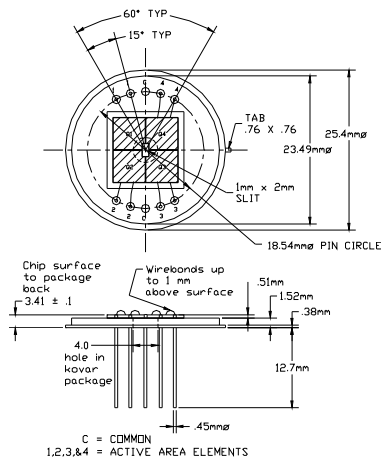
PS5



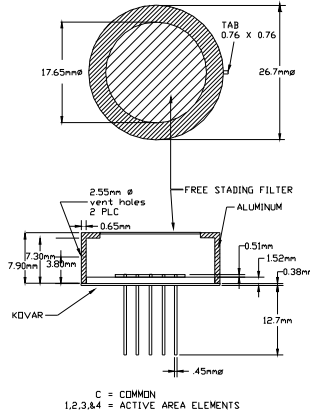
U = UNCONNECTED OPEN
C = COMMON PINS

PS1

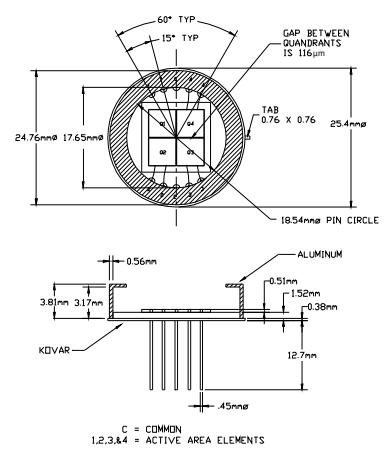
All units in mm
General package tolerances (unless otherwise specified):
.xx ± .4 mm ± .1 mm Angular ± 2



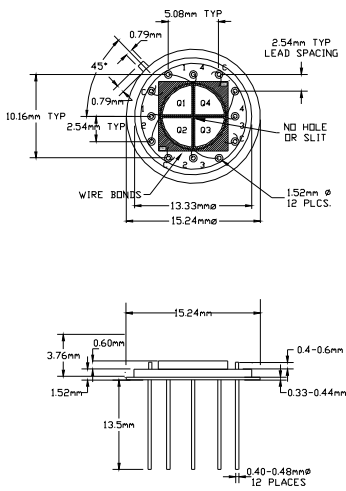
PS2



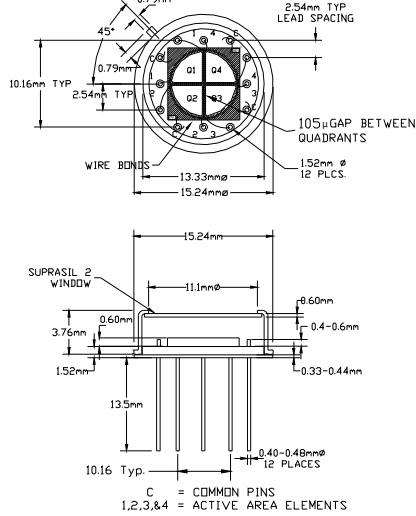
PS2 with Free Standing Filter



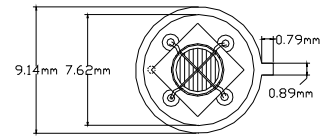
PS1



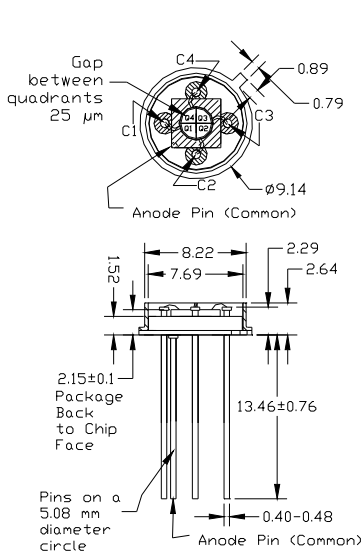
*MTO8



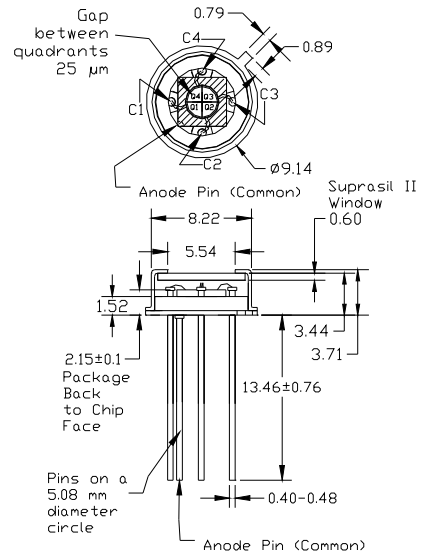
MTO8S



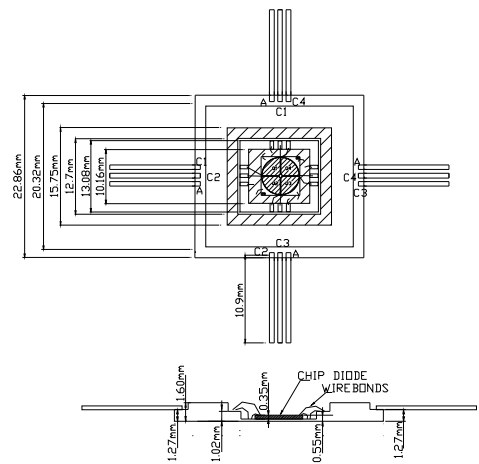
PS4



PS4C

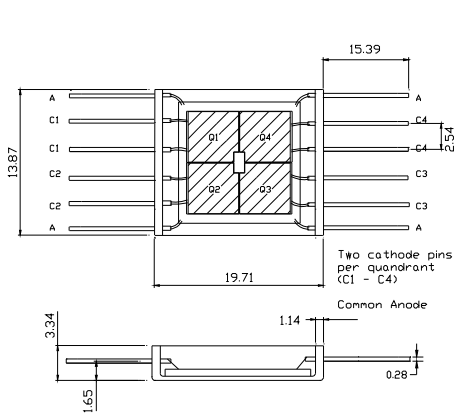


PS4S

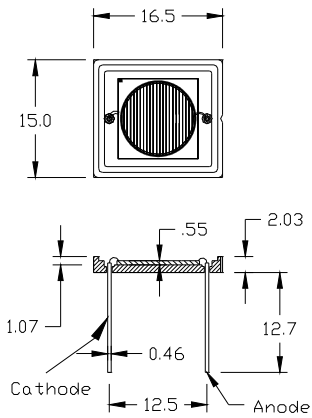


PS1LP

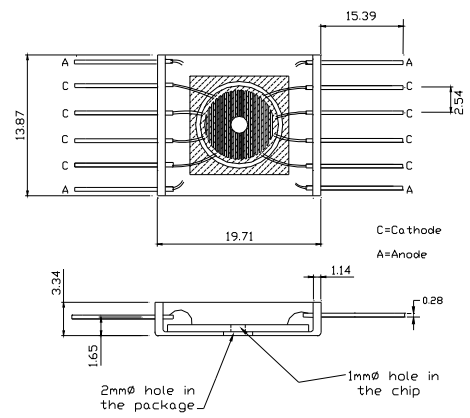
*The package has opening appropriate with the central opening in the chip
 All units in mm
 General package tolerances (unless otherwise specified):
 .xx ± .4 mm ± .1 mm Angular ± 2



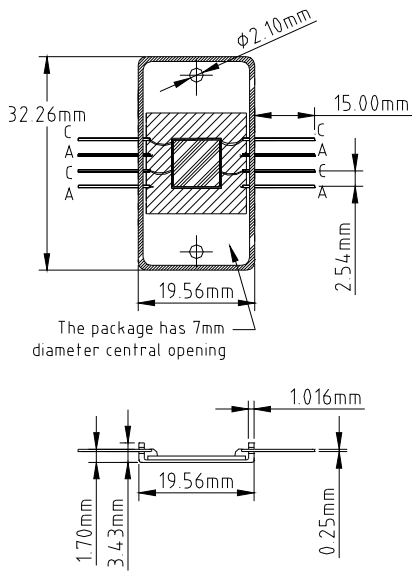
PS2LP



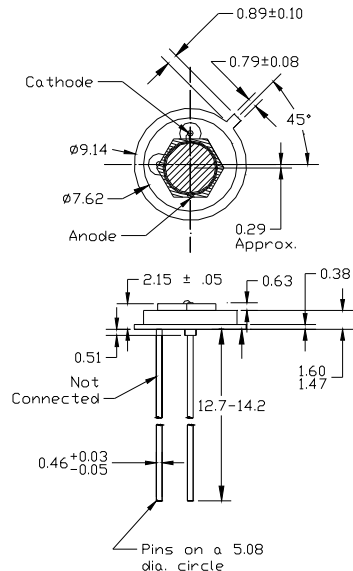
C63



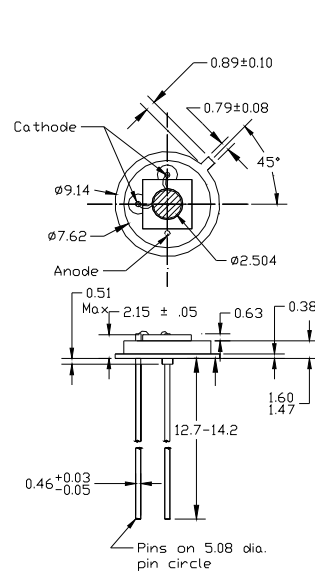
M63LP



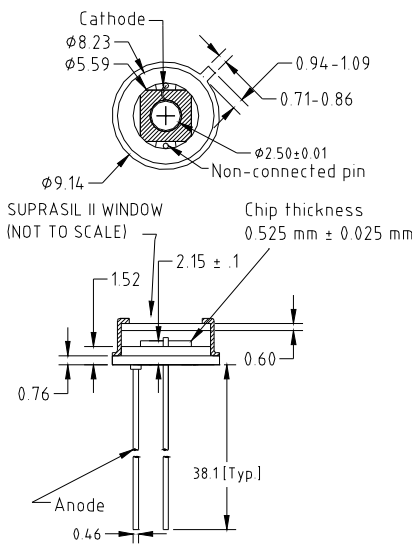
M36



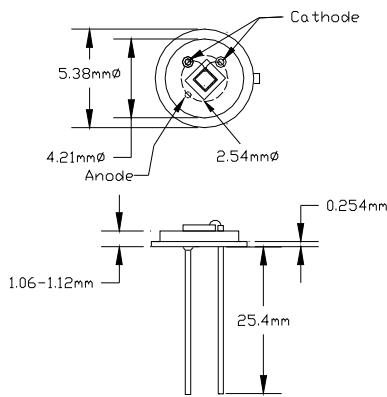
TO5A



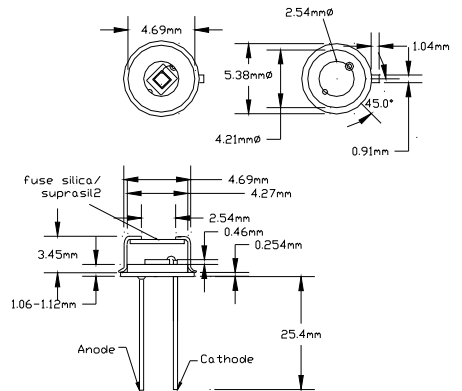
TO5B



TO5S

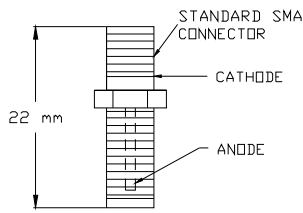
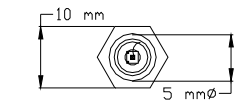


TO46

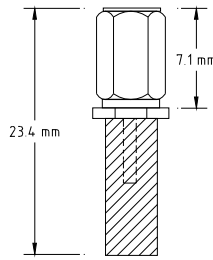
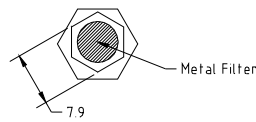


TO46S

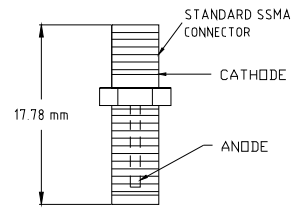
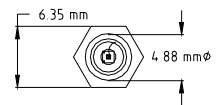
All units in mm
 General package tolerances (unless otherwise specified):
 .xx ± .4 mm ± .1 mm Angular ± 2



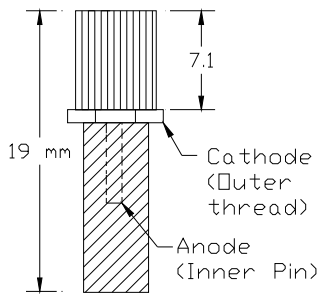
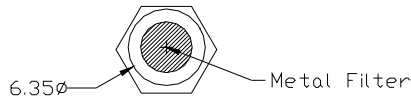
SMA



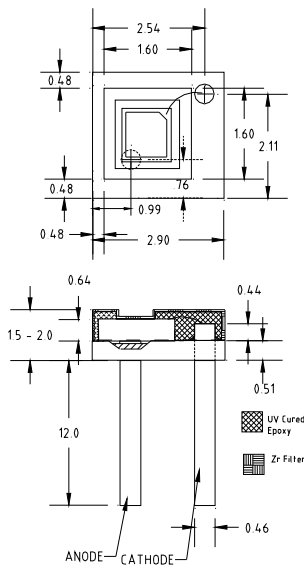
SMA with Free Standing Filter



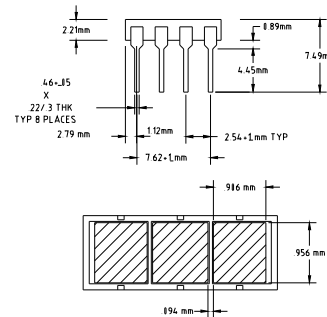
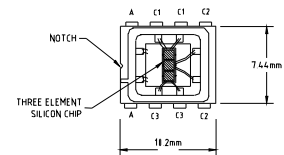
SSMA



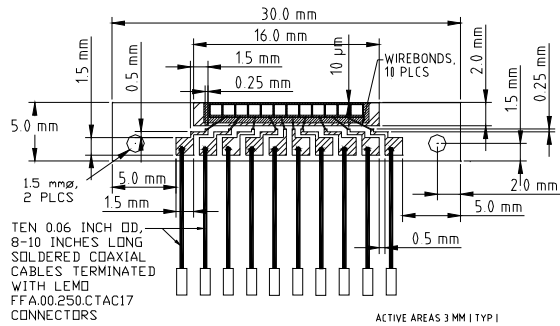
SSMA with Free Standing Filter



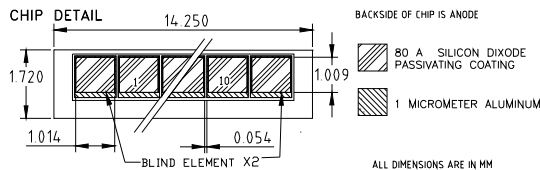
CHS5



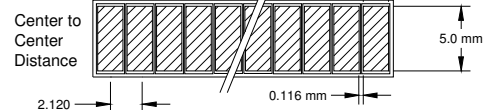
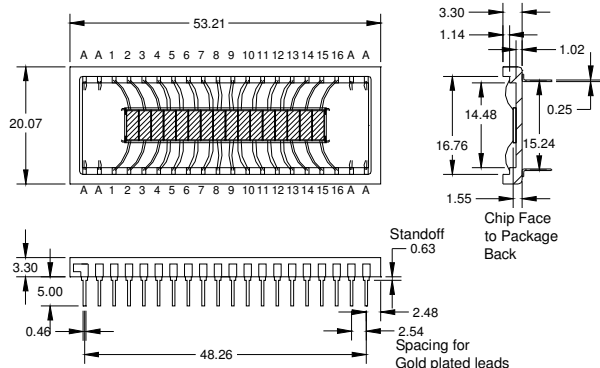
C3EL



TEN 0.06 INCH OD, 8-10 INCHES LONG SOLDERED COAXIAL CABLES TERMINATED WITH LEMO FFA.00.250.CTAC17 CONNECTORS

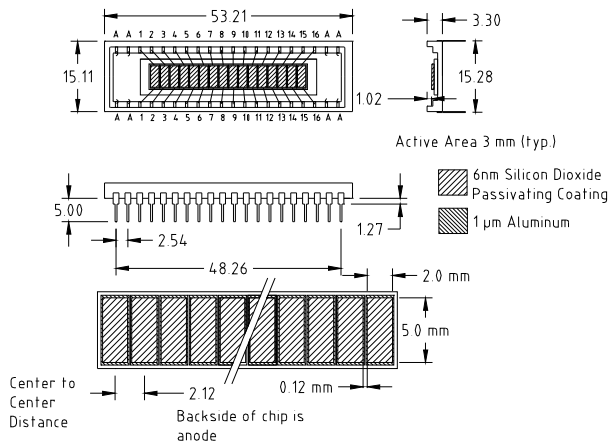


C10EL

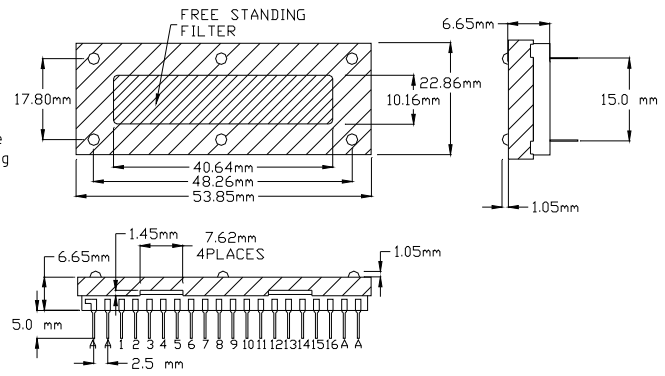


C16ELO

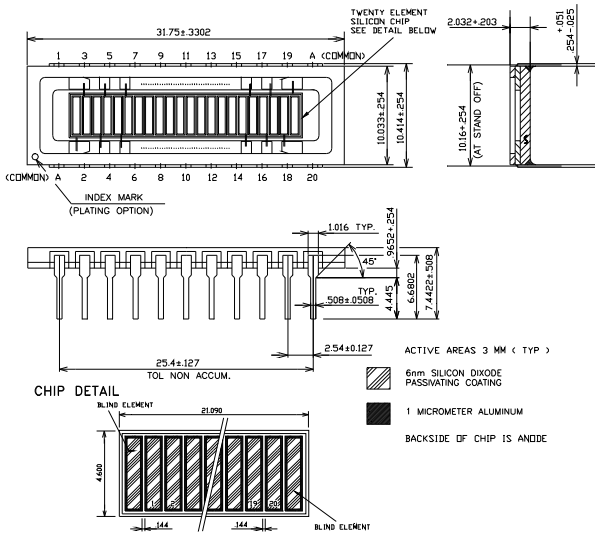
All units in mm
 General package tolerances (unless otherwise specified):
 .xx ± .4 mm ± .1 mm Angular ± 2



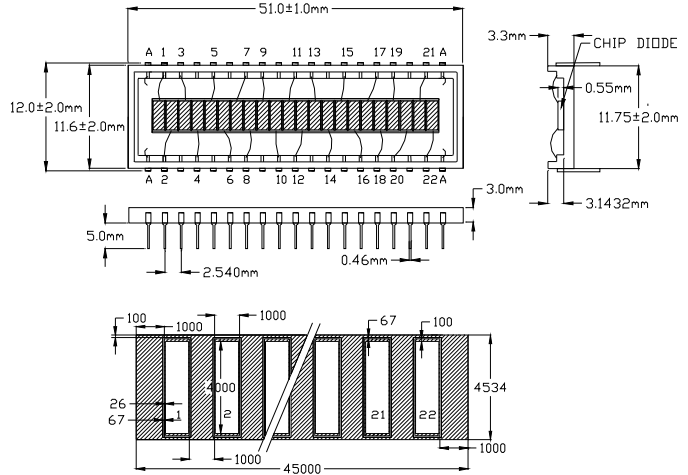
C16EL



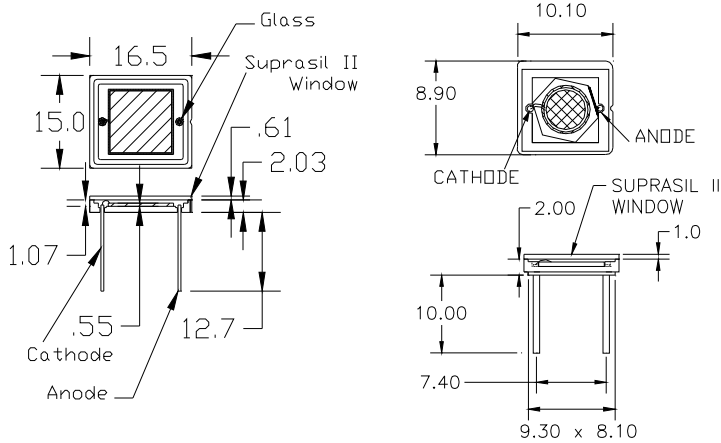
C16ELO with Free Standing Filter



C20EL

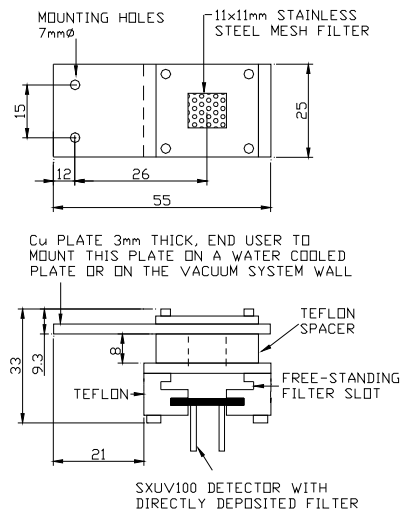


C22EL



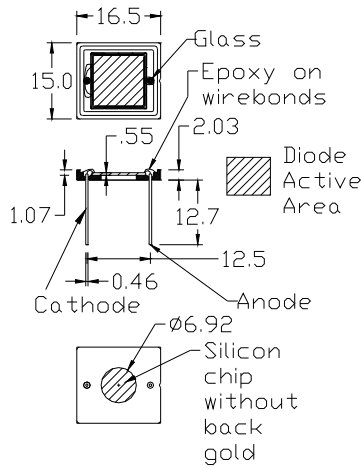
C100S

C20S

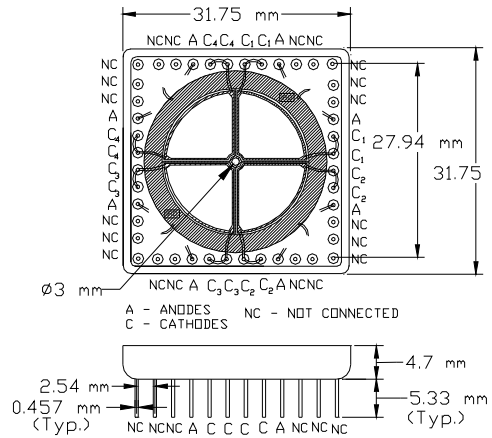


100mj

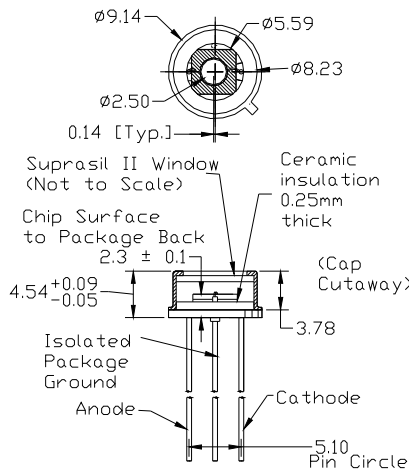
All units in mm
 General package tolerances (unless otherwise specified):
 .xx ± .4 mm ± .1 mm Angular ± 2



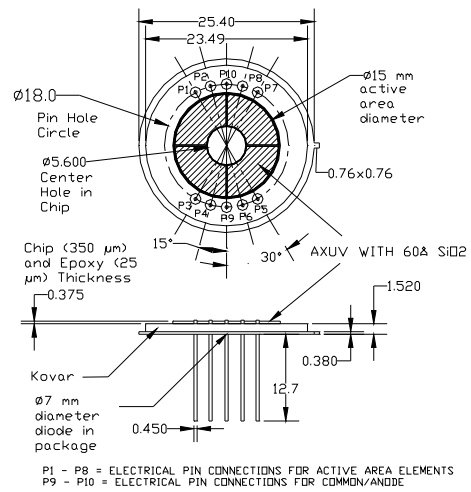
C100GX



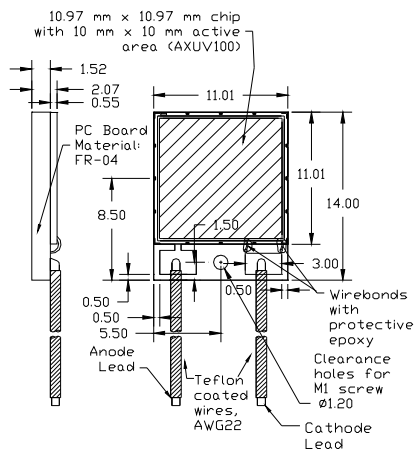
PS8



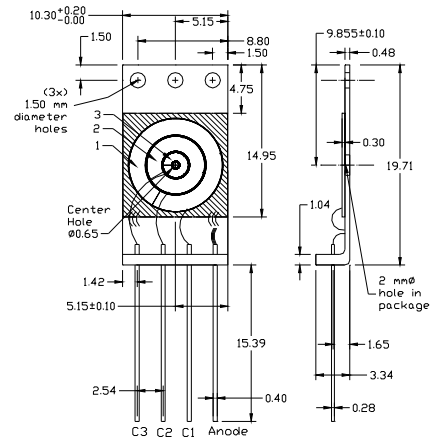
TO5SI



PS7

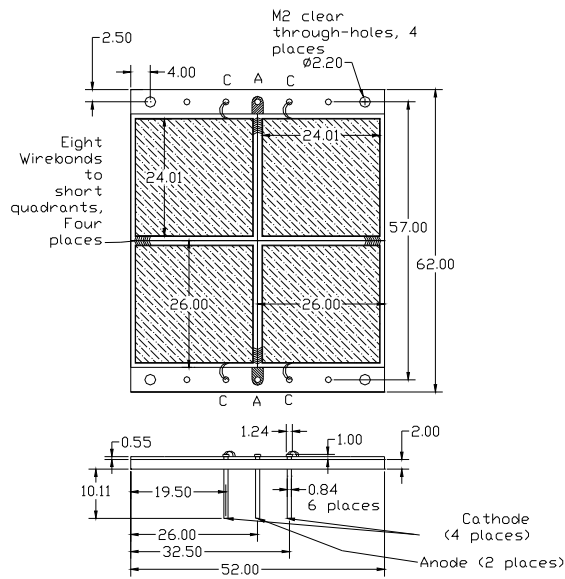


PC100

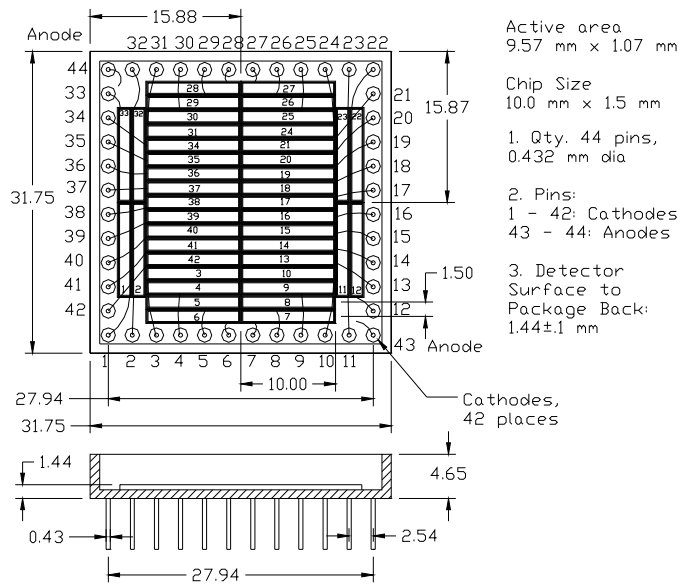


M3CR

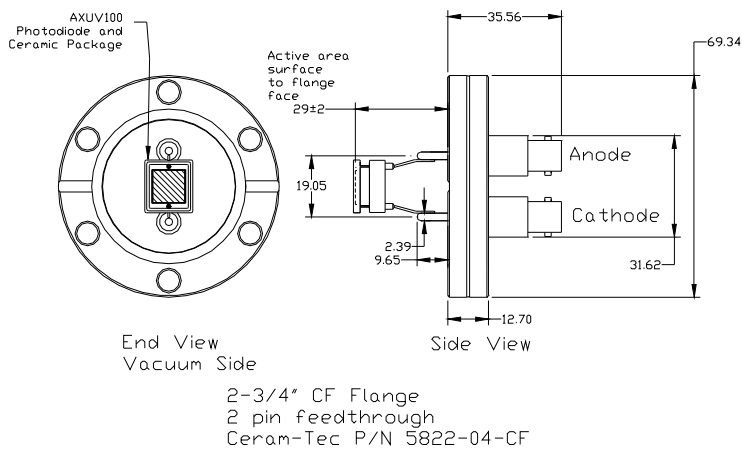
All units in mm
 General package tolerances (unless otherwise specified):
 .xx ± .4 mm ± .1 mm Angular ± 2



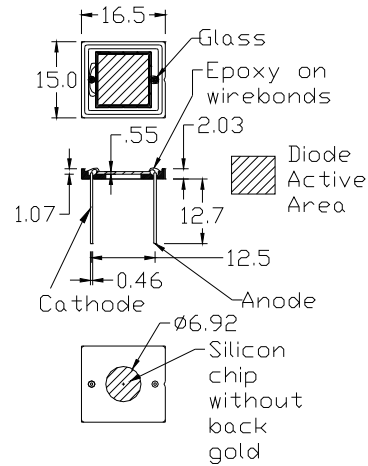
C2300



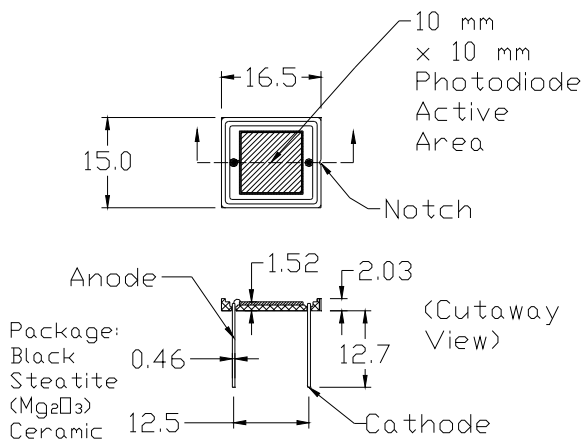
M42EL



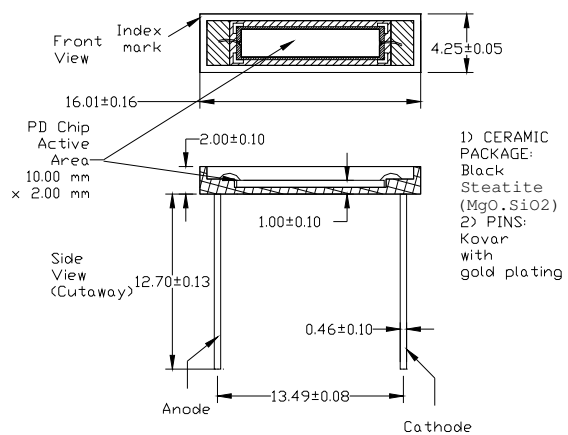
C100F



C100GX



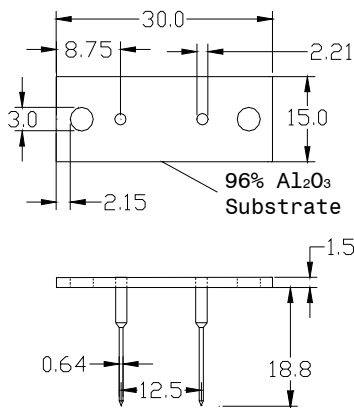
C100PN



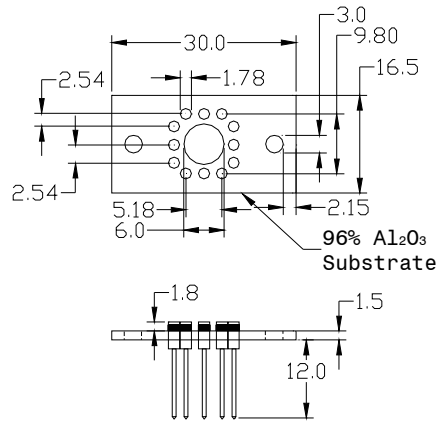
C19

All units in mm
 General package tolerances (unless otherwise specified):
 .xx ± .4 mm ± .1 mm Angular ± 2

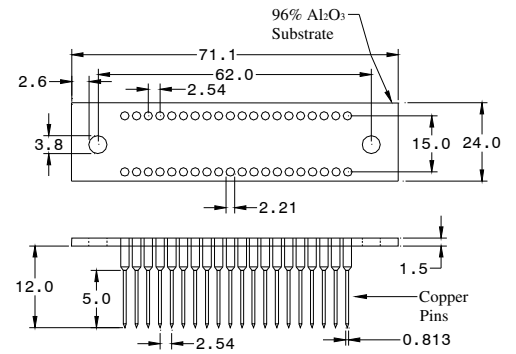
Ceramic Sockets



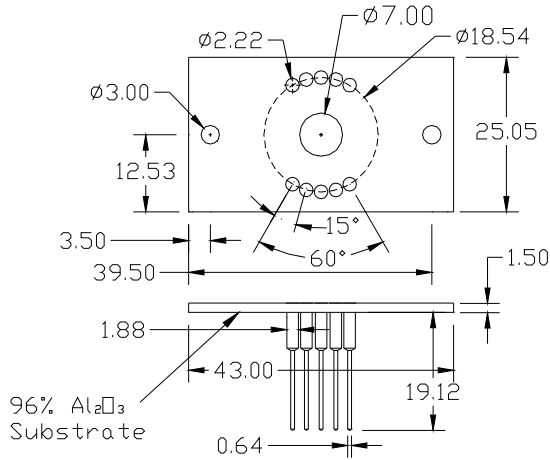
AXUV100CS



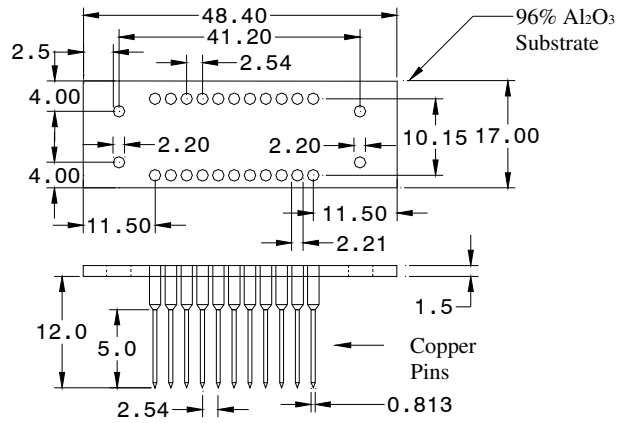
AXUVPS1ACS



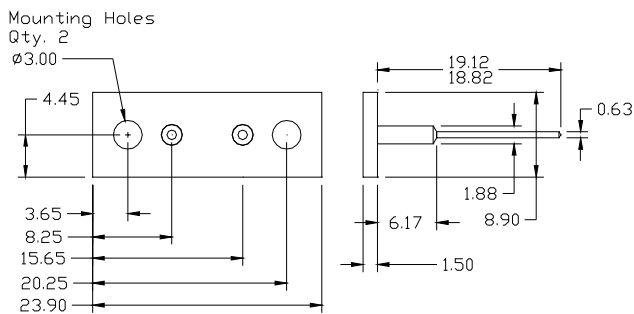
AXUV16ELCS



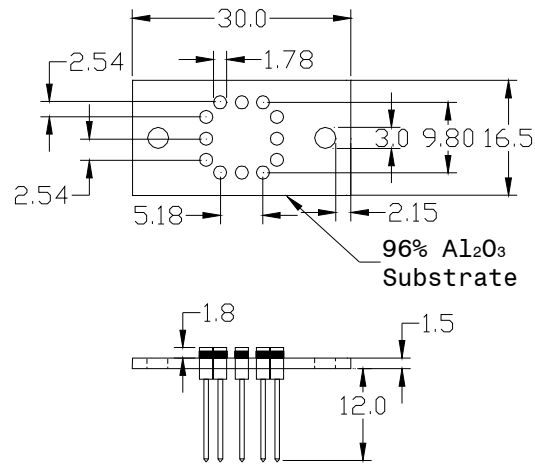
AXUVPS3CS



AXUV20ELCS



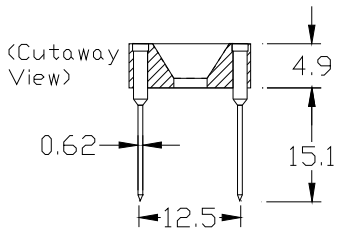
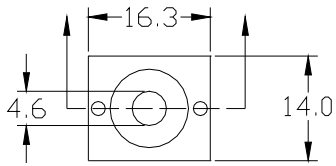
AXUV20ACS



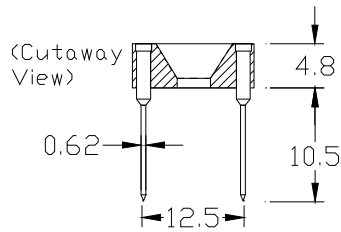
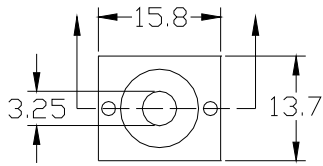
AXUVPS6CS

- 1) All dimensions are in mm
- 2) Cut device leads for better fit if necessary

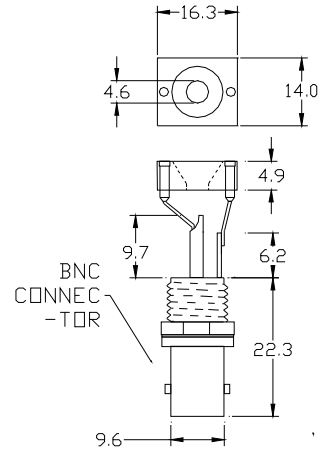
Teflon Sockets



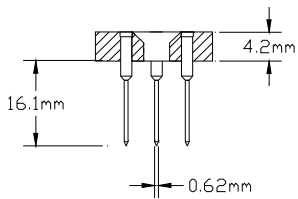
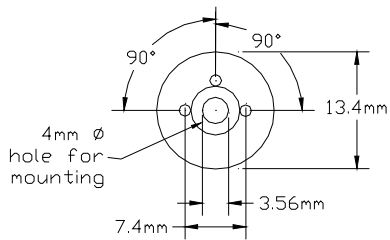
AXUV100TS



AXUV100TSA

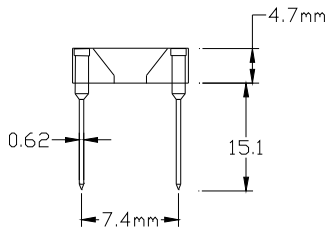
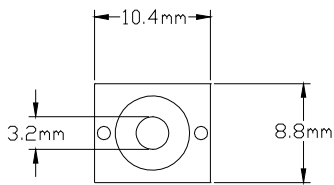


AXUV100TS/BNC

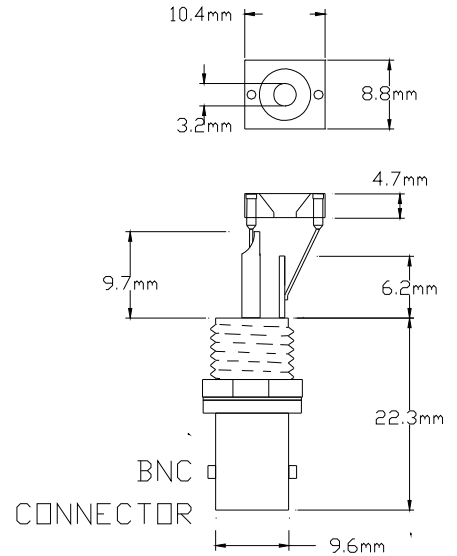


NOTE: MOUNTING HOLE MADE FOR THE 8-32 SCREW SIZE

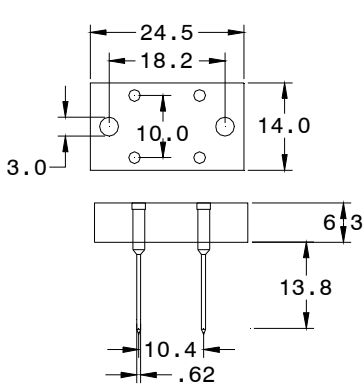
AXUV20TS



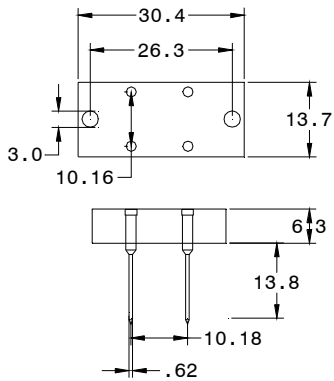
AXUV20ATS



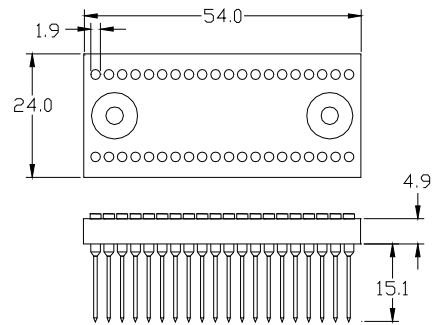
AXUV20ATS/BNC



AXUV20HE1TS

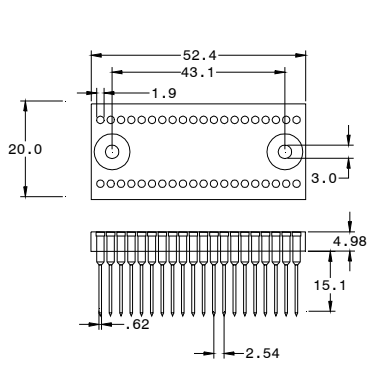


AXUV96TS

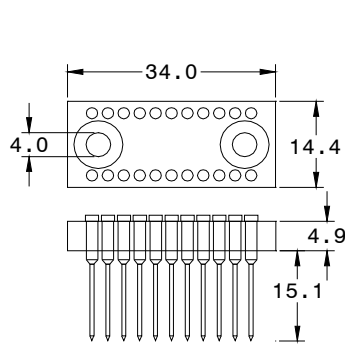


AXUV16ELOTS

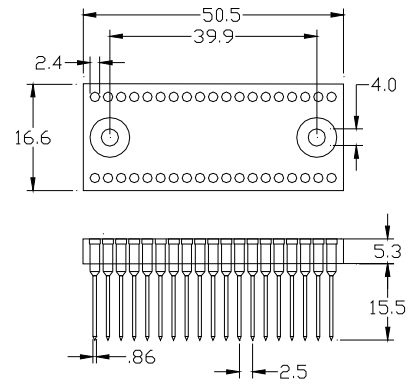
- 1) All dimensions are in mm
- 2) Cut device leads for better fit if necessary



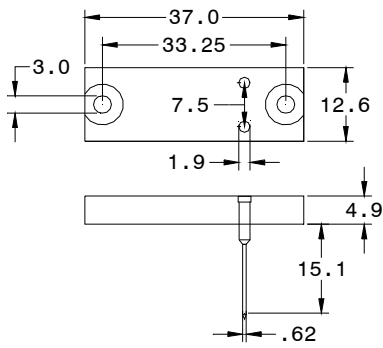
AXUV16ELTS



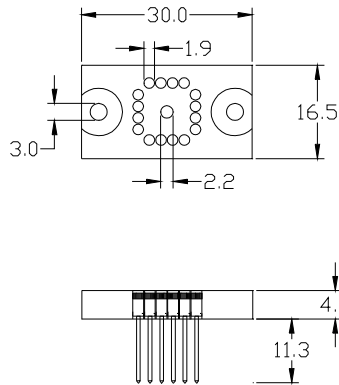
AXUV20ELTS



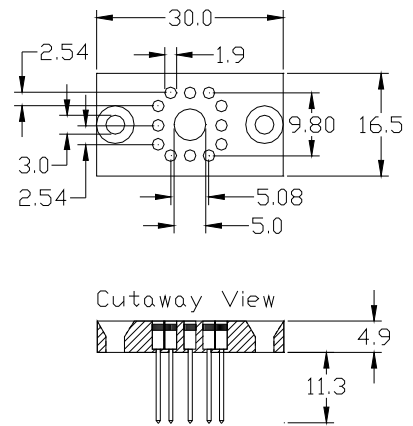
AXUV22ELTS



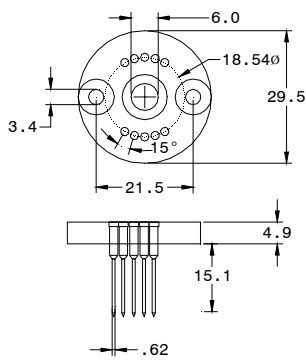
AXUVSP2TS



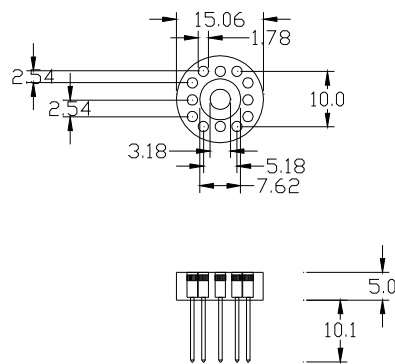
AXUVPS1TS



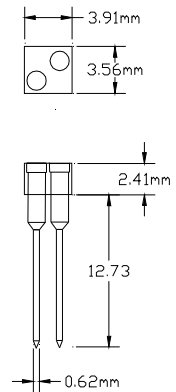
AXUVPS1ATS



AXUVPS2TS

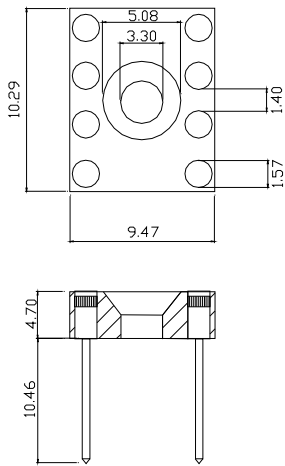


AXUVPS6TS

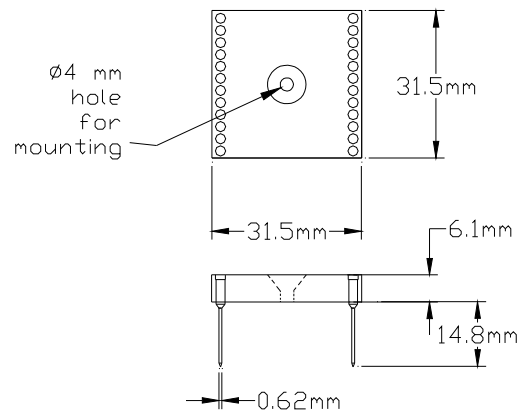


AXUVHS5FILTER

- 1) All dimensions are in mm
- 2) Cut device leads for better fit if necessary

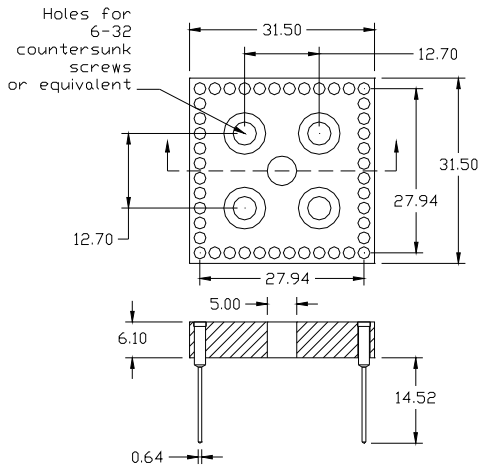


AXUVELATS

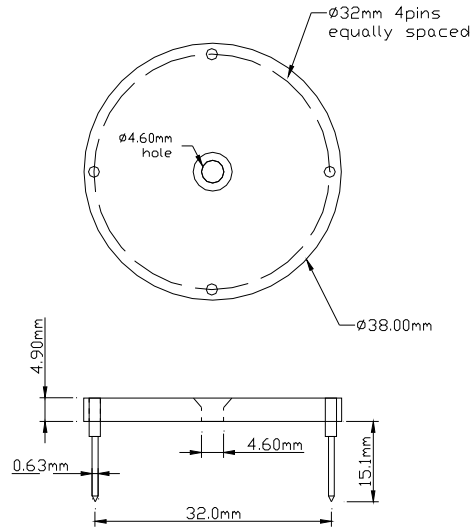


NOTE: MOUNTING HOLE MADE FOR THE 8-32 SCREW SIZE

AXUV576/600MTS



AXUVPS8TS



AXUV576CTS

- 1) All dimensions are in mm
- 2) Cut device leads for better fit if necessary

Electronics

Light pulse energy is quite often determined by measuring the peak voltage generated across the photodiode. As the diode capacitance (which determines the peak voltage) changes with the injection level because of the carrier diffusion effects, we believe that this method is inferior to that of pulse energy determination by measuring the photogenerated charge. Therefore, all electronics developed by IRD measure the charge generated by the pulse radiation.

The BT250 described on this page can be used with AXUV/SXUV/UVG photodiodes if the impinging pulse energy is greater than 10 nJ. For the lower pulse energies, the PA100 amplifier described on the following page should be used. A further extension of the PA100 amplifier is the PA13 pulse energy measurement system, described on page 26.

During the CW XUV radiation measurement, general purpose electrometers are used to measure the current generated by the photodiodes. They are commonly used with IRD photodiodes around a synchrotron light source. However, the relatively large size of many commercial electrometers makes it difficult to locate them close to the detector. The long interconnecting cables can pick up significant amounts of noise from electromagnetic interference and from mechanical vibration.

The AXUV100HYB1 amplifier shown on page 27 is a high vacuum compatible current-to-voltage converting amplifier

developed specifically for use with the AXUV100 and AXUV20 photodiodes. The combination of the detector/amplifier hybrid can be used to measure small photogenerated currents with resolutions of 10 fA and dynamic ranges of four orders of magnitude. The AXUV100HYB1 consists of a very low noise operation amplifier with a fixed 10G-ohm feedback resistor. All components are low tolerance resulting in consistent current-to-voltage transfer characteristics with minimal offset voltage.

If more dynamic range is needed, the AXUV100HYB1 can be ordered with variable-feedback resistors model #AXUV100HYB1. A similar amplifier is available for AXUV20A diode model #AXUV20AHYB1/V.

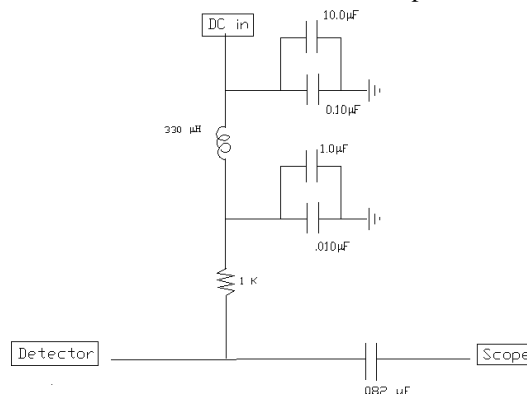
The amplifier for the AXUV16EL array is described on page 28. This amplifier uses four quadrant operational amplifiers with a built-in AXUV16EL chip. The AMP16 provides a less expensive version without the integrated AXUV16EL chip.

AXUV100HYB1/V, AXUV20AHYB1/V and the AXUV16ELOHYB1 amplifiers have been used in vacuum systems with pressures as low as 10^{-7} torr. Because of the electronic components involved, these amplifiers should only be vacuum baked, if necessary, to a maximum temperature of 100°C.

BT250 Bias Tee

When measuring energy of light pulses with the IRD photodiodes, it is recommended that a reverse bias be used. These photodiodes will become nonlinear for pulse energies greater than about a nJ if used without bias. Applying a reverse bias will raise the saturation threshold to higher levels. The BT-250 is a low noise bias insertion tee with a DC blocking capacitor that was designed specifically for use with the AXUV/SXUV/UVG series photodiodes. The BT250 is rated for up to 250V applied bias and an optional BT500 is available with voltage rating up to 500 V.

The BT250 has 3 ports connected with BNC cables to a digital oscilloscope, DC power supply and photodiode. The BT250 can be connected to a common ground with a banana plug. Be sure the detector is reversed biased. To check if the detector is reverse-biased, slowly increase the bias voltage and verify that the current is not rapidly increasing. If it is, switch the polarity on the power supply. (Note: the detector may be damaged by a forward bias.) The amount of bias should not exceed the breakdown voltage of the detector. It is estimated that the measured output of the BT-250 is approximately 5% less than the actual output of the diode due a loss in the bias tee.



Schematic of BT250

PA100 Pulse Amplifier

Description

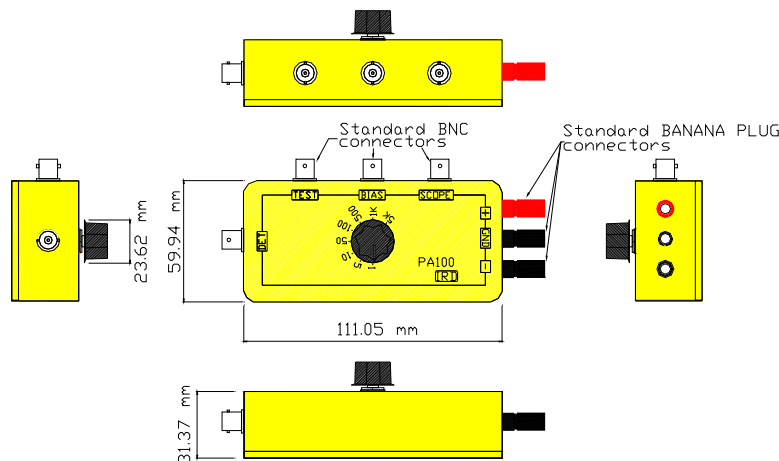
The PA100 is a pulse amplifier used to counteract the effects of attenuating signal cables on small signals generated from photodiodes. The PA100 accomplishes this function by isolating the detected photodiode signal from the line inductance and capacitance typical of coaxial signal cables. This isolation function allows very small photodiode signals (on the order of 10fC) to be transmitted over several feet of common 50 ohm coaxial cables without being corrupted by noise pick-up.

Integral to the PA100 amplifier is a high quality 2-pole filter used to reduce power supply coupled noise on the amplifier output and an internal detector bias network used to supply a

bias of 0-50V to the detector

Features

- AC coupled detector bias network for photodiodes with up to 1 μ A of dark current at 50V and up to 500 nF capacitance. Bias network is bipolar.
- Internal power supply filter network.
- Selectable gains of 1, 5, 10, 50, 100, 500, 1000 and 5000 X. If requested, the gain can be remotely selected.
- Integral test capacitor to facilitate charge injection input for calibration.



Specifications

Parameter	Conditions	Minimum	Typical	Maximum	Units
Detector Capacitance	As attached to PA100	-	-	500	nF
Detector dark current leakage	As attached to PA100	-	-	1	μ A
Detector Bias Voltage	As attached to PA100	0	-	50	V
Minimum Charge Detection Limit	As attached to PA100	7	10	20	fC
Risetime	Gain = 5000		25		μ s
Maximum Pulse Width	As attached to PA100	-	-	62	ms
Noise Figure	All bands		16	64	$nV/(Hz)^{1/2}$
Test Capacitor	Integral to PA100	9	10	11	pF
Peak output	Saturation distortion		4		V
Power Supply	Dual	+/- 6	+/- 12	+/- 17	V

PA100V Pulse Amplifier

Description

The PA100V amplifier consists of three main components which are a ceramic board PA100V pre-amp, PA100V control box and a ceramic transition board. The pre-amp is a vacuum compatible, programmable gain amplifier and houses the photodiode. The ceramic transition board connects the pre-amp to the vacuum side of standard 15 pin sub-miniature d-shell feedthrough. The gain control and connections to signal, power etc. of the pre-amp are provided by the control box which can be mounted directly on the atmosphere side of the vacuum system wall. A PA13 sampler board provides power for the whole circuit and also provides a voltage proportional to the charge developed in the detector.

The pre-amp board can accept AXUV/SXUV 20 and AXUV/SXUV 100 devices. The detectors can be reverse biased up to 12 Volts.

The PA100V is a pulse amplifier used to counteract the effects of attenuating signal cables on small signals generated from photodiodes. The PA100V accomplishes this function by isolating the detected photodiode signal from the line inductance and capacitance typical of coaxial signal cables.

This isolation function allows very small photodiode signals (on the order of 10fC) to be transmitted over several feet of common 50 ohm coaxial cables without being corrupted by noise pick-up.

Features

- AC coupled detector bias network for photodiodes with up to 1 μ A of dark current at 12V and up to 500 nF capacitance. Bias network is bipolar.
- Internal power supply filter network.
- Selectable gains of 1,5,10,50,100,500, 1000 and 5000 X. If requested, the gain can be remotely selected.
- Integral test capacitor to facilitate charge injection input for calibration.
-

PA100V Specifications

Parameter	Conditions	Minimum	Typical	Maximum	Units
Detector Capacitance	As attached to PA100	-	-	500	nF
Detector dark current leakage	As attached to PA100	-	-	1	μ A
Detector Bias Voltage	As attached to PA100	0	-	50	V
Minimum Charge Detection Limit	As attached to PA100	7	10	20	fC
Risetime	Gain = 5000		25		μ s
Maximum Pulse Width	As attached to PA100	-	-	62	ms
Noise Figure	All bands		16	64	nV/(Hz) ^{1/2}
Test Capacitor	Integral to PA100	9	10	11	pF
Peak output	Saturation distortion		4		V
Power Supply	Dual	+/- 6	+/- 12	+/- 17	V

PA13: Multi-channel System for Pulse Energy Measurement

The PA13 detection system is an instrument that measures the illumination intensity in a pulsed environment. This system produces an output voltage that is proportional to the intensity of radiation incident on the IRD photodiodes. This is achieved by charge amplification and integration. The PA13 incorporates a self-test feature that allows users to exercise the functionality of the detection system without requiring illumination of the detector.

The PA13 Multi-channel Pulse Detection System contains up to 10 identical channels which include the following instrumentation:

(1) a preamplifier board which amplifies the charge produced from pulse radiation incident on the photodiode

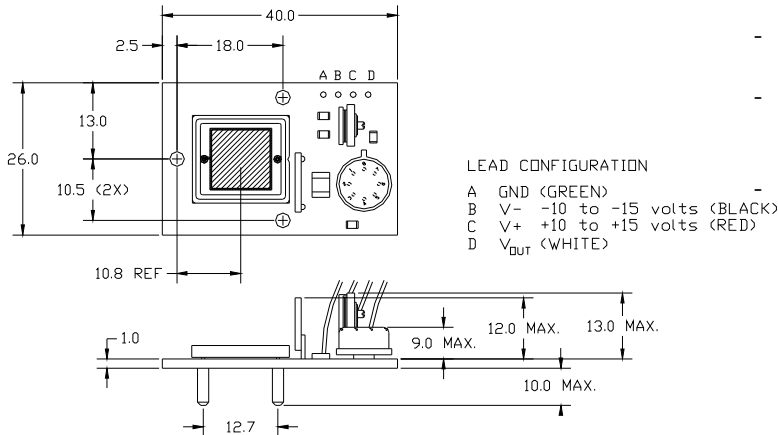
(2) a driver board which provides the power to drive the signal over long cables

(3) a sampler board that samples the pulse produced by the preamplifier and provides an output voltage proportional to the input charge. The sampler board also provides power to the entire detector chain. Following table describes specifications of the PA13 system.

Specifications

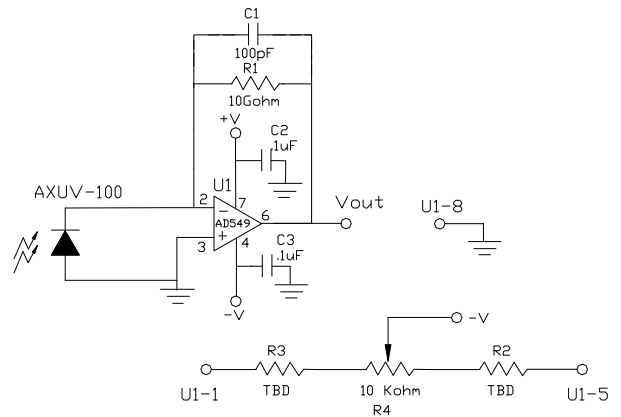
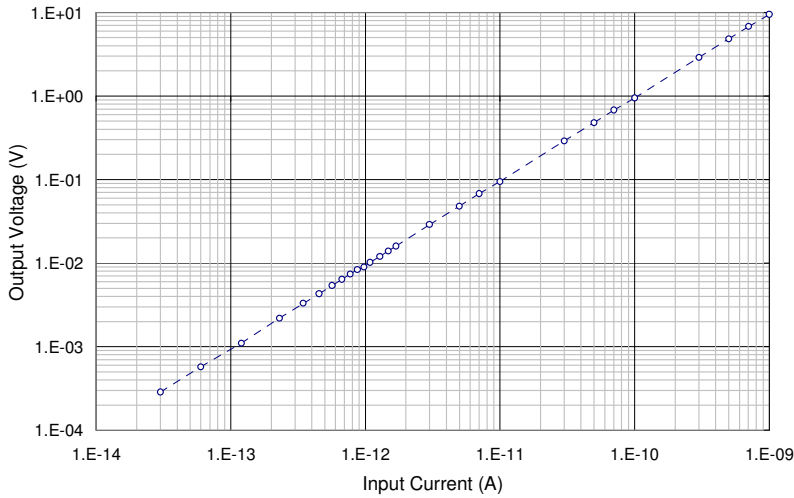
Parameter	Conditions	Min	Typ	Max	Units
Detector Bias Voltage		0	10	12	V
Minimum Charge Detection Limit	High Gain	-	1	2	pC
Maximum Charge Detection Limit	High Gain		100	110	pC
Maximum Charge Detection Limit	Low Gain		1000	1100	pC
Maximum Pulse Width	Low gain/High Gain	30	50/150	75/200	μs
Acceptable Source Sample Rate	All Gain ranges	10	1K	2K	Hz
Noise Figure	All bands (unsampled)	>8	16	64	nV/ (Hz) ^{1/2}
Test Capacitors	Integral to each channel	9	10	11	pF
Max Sampled Output	High Gain, 100 pC test charge		10	10.5	V
Max Sampled Output	Low Gain, 100 pC test charge		1.2	1.4	V
Power Supply Input Voltage	50 – 60 Hz	120	220		V
Total System Operating Current	Per Channel (sampler, buffer and pre-amp)		120		mA
Preamp power Supply Current	V = +/- 12 V		3.75		mA
Buffer Power Supply Current	V = +/- 12 V		3.0		mA
Preamp Power Dissipation			45		mW
Buffer Power Dissipation			36		mW
System Operating Current	All 10 channels		1.2		A

AXUV100HYB1

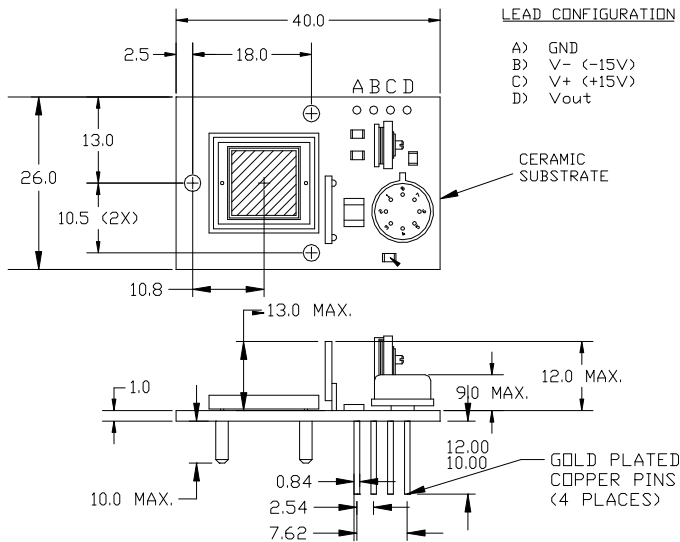


- Operational amplifier on a ceramic board.
- Available with UHV compatible version (AXUV100HYB1V).
- Amplifier accepts UVG100, AXUV100 and SXUV100 type packages.

Typical Transfer Characteristics of AXUV100HYB1

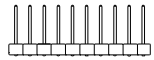
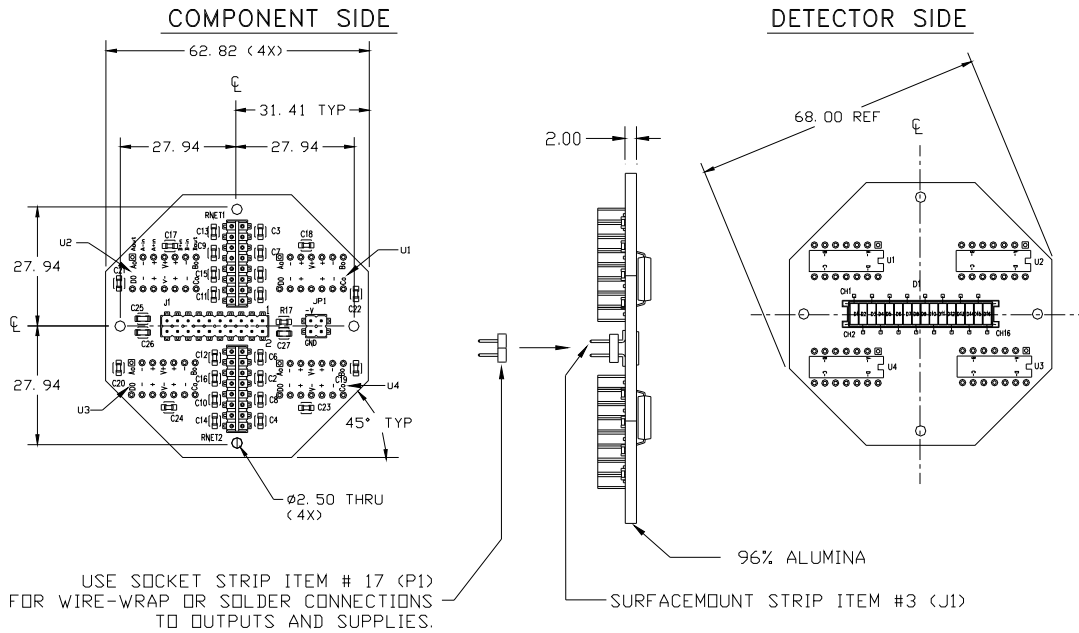


AXUV100HYB1VCu



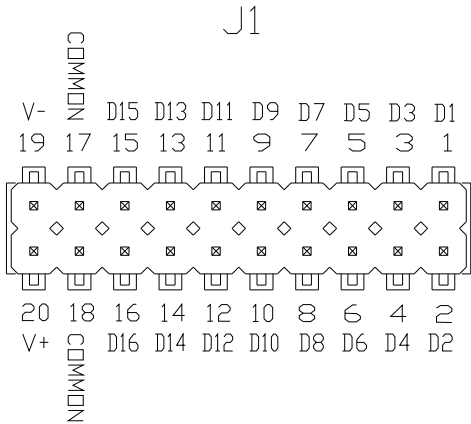
- Vacuum compatible amplifier board with extended pins for simplified electrical hookup.
- Amplifier accepts UVG100, AXUV100 and SXUV100 type packages.

AXUV16ELOHYB1

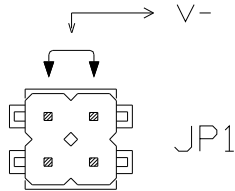


P1

- NOTES: 1) PLEASE DO NOT SOLDER
2) DO NOT CLEAN THIS ASSEMBLY
3) DO NOT TOUCH THE TOP SURFACE OF
THE PHOTODIODE



BIAS JUMPER



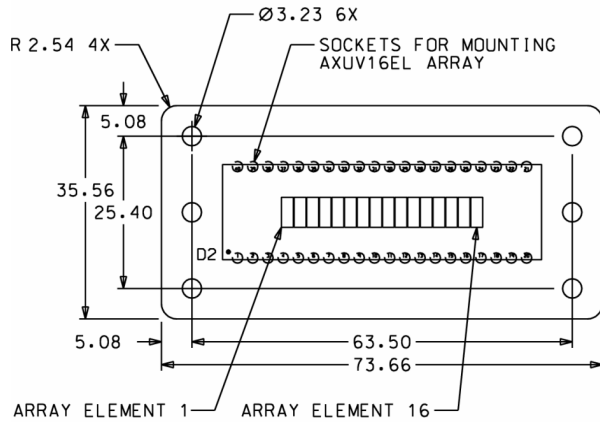
- NOTES: 1. APPLY -10 TO -15 VOLTS DC TO J1 PIN #19
2. APPLY +10 TO +15 VOLTS DC TO J1 PIN #20
3. J1 PINS #17 & PIN #18 ARE BOTH TIED TO COMMON.
4. D1 THROUGH D16 CORRESPOND TO THE SIXTEEN CHANNELS OF THE AXUV-16ELO PHOTODIODE CHIP.
5. BIAS JUMPER IS CONNECTED TO OPERATE THE PHOTODIODE ARRAY AT 15 VOLTS REVERSE BIAS

ELECTRICAL SPECIFICATION (25 °C)

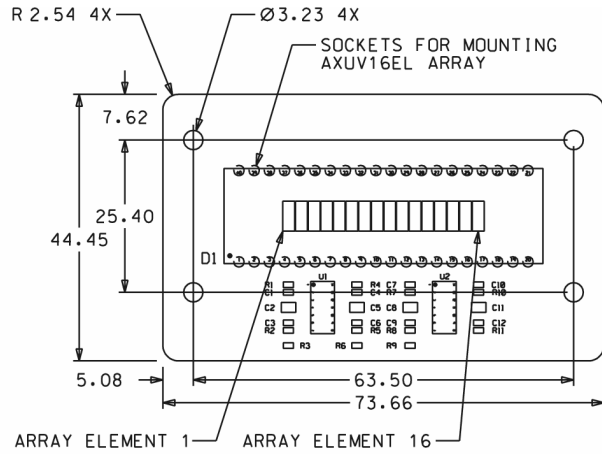
TRANSFER FUNCTION	100 kV/A, +/- 1%
BANDWIDTH	400 kHz
OUTPUT OFFSET VOLTAGE	60 mV
OUTPUT NOISE VOLTAGE	7.9 $\mu\text{V}/\sqrt{\text{Hz}}$

AMP16: Amplifier for AXUV16EL Array

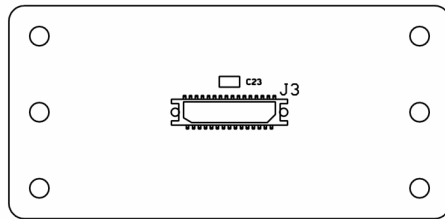
The AMP16 is a 16-channel vacuum compatible amplifier on a ceramic board designed for use with the AXUV16EL array. The AMP16 is a less expensive version of the AXUV16ELOHYB1, with an added advantage of versatility in mounting the array. The AXUV16EL array may be mounted directly to the main board or it may be placed on a dedicated remote-mounting board, connected to the main board by a 20 cm cable (Hirose 31-pin cable, part #DF9-31P-1(20)). Output signal is via a female 37-pin D-subminiature connector on the main board, which connects to a standard D-subminiature connector (Digikey part #A2046-ND or equivalent).



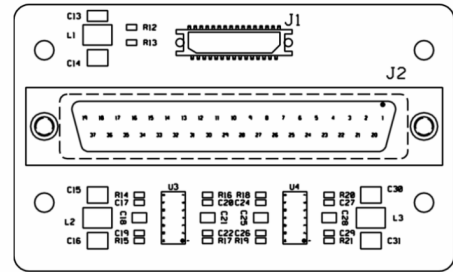
REMOTE BOARD, FRONT



MAIN BOARD, FRONT



REMOTE BOARD, REAR



MAIN BOARD, REAR

DIMENSIONS IN MM

SPECIFICATIONS

(ROOM TEMPERATURE)

BOARD COMPOSITION	96% AL_2O_3
DETECTOR HEIGHT (FROM BOARD SURFACE)	8.5 MM
POWER SUPPLY	+/- 15 VOLTS
BANDWIDTH	600 KHZ
TRANSFER FUNCTION	100 kV/A, $\pm 1\%$
OUTPUT OFFSET VOLTAGE	60 mV
OUTPUT NOISE VOLTAGE	$7.9 \mu V/Hz^{1/2}$

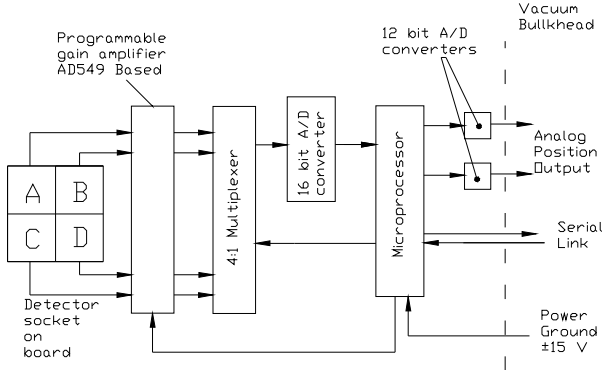
QSP1 Quadrant Signal Processor

The quadrant signal processor (QSP1) is a position sensing instrument designed to work with all the quadrant 12 pin TO-8 packaged devices (like AXUVPS1A, SXUVPS6 etc.) The instrument is designed to amplify photogenerated currents down to the 1 pA level, acquire data from the four quadrants, and determine the beam position illuminating the detector. The entire package is 7.62 cm diameter and fits into a Newport SB80 lens mount.

This instrument determines the beam position from a high performance amplifier subsystem in conjunction with an on-board microprocessor. It is designed to collect quadrant signals for CW illumination. The system acquires data from the quadrants, processes it, and reports the resultant position. This is achieved at a rate of approximately one sample per second.

The QSP1 design is unique and has several advantages over the other quadrant signal processors available. The detector signal normalization is performed digitally. This is unaffected by noise at low illumination levels on the detector. This means that the reported position is unaffected by wide (orders of magnitude) variations in illumination intensity. This level of stability can not be performed solely by analog means used by other quadrant processors on the market. The reported measurements in QSP1 can be collected digitally avoiding the purchase of additional data collection hardware.

The QSP1 has several built-in test programs to help in debugging the instrument operation as well as assisting-in determining the validity of the collected data.



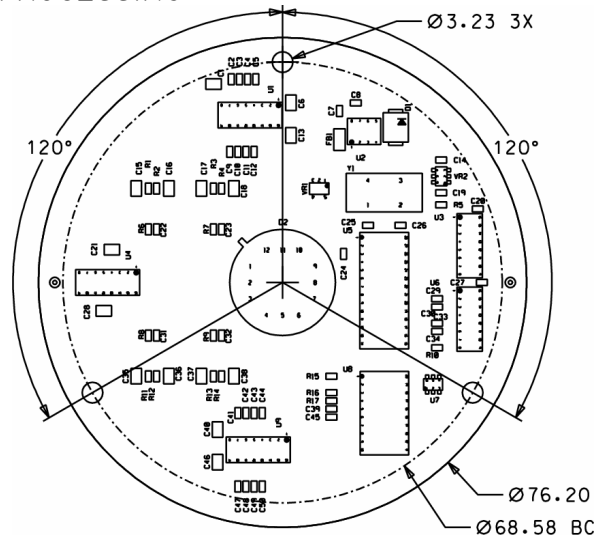
- Microprocessor Performs the following function:
- 1) Digitizes individual quadrant cell currents
 - 2) Corrects for dark currents (digitally)
 - 3) Verifies that all cells are collecting data
 - 4) Perform center calculation (digitally)
- $$X = kx((A+C)-(B+D))/(A+B+C+D)$$
- $$Y = ky((A+B)-(C+D))/(A+B+C+D)$$
- 5) Send data via serial link
 - 6) Load D/A converters with results

Gain is adjusted via the serial port

SPECIFICATIONS (ROOM TEMPERATURE)

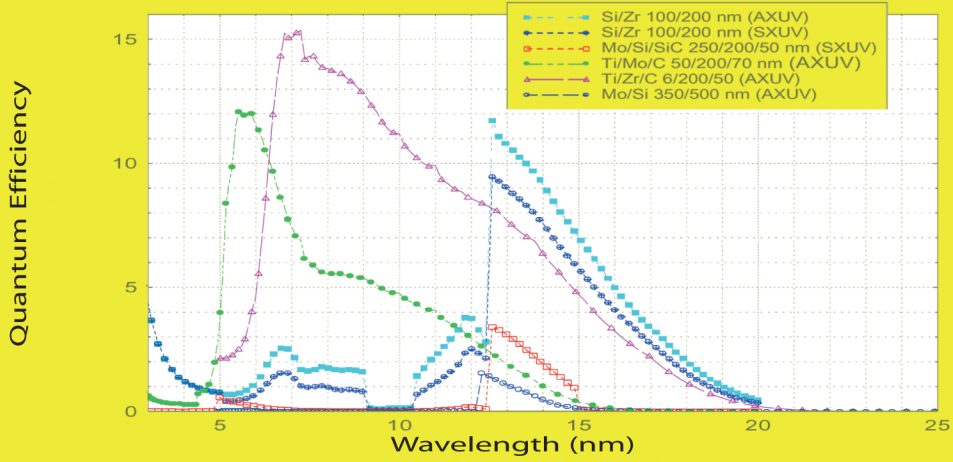
POPULATED BOARD THICKNESS	12 MM
BOARD MATERIAL- PC BOARD	FR4
DETECTOR HEIGHT (FROM BOARD SURFACE)	6 MM
BANDWIDTH RESPONSE	2-10 HZ
SCALES	.1, 1, 10, 100 PA/V
SIGNAL RANGE	0 - 4.095 VOLTS
SIGNAL RESOLUTION	12 BITS CENTERED AT 2.048 VOLTS
DATA CONNECTION	SERIAL
POWER SUPPLY	+/- 15 VOLTS
POWER DISSIPATION	< 1 WATT

SCHEMATIC OF DATA PROCESSING

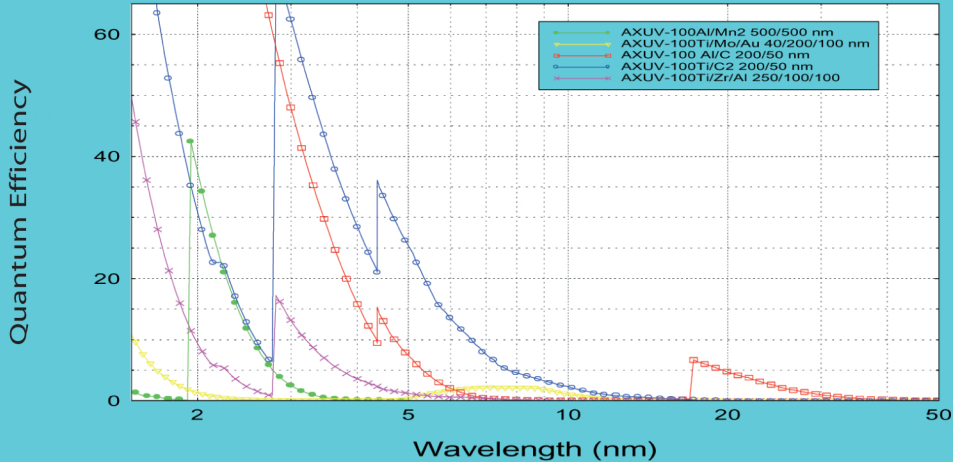


FRONT LAYOUT OF QSP1

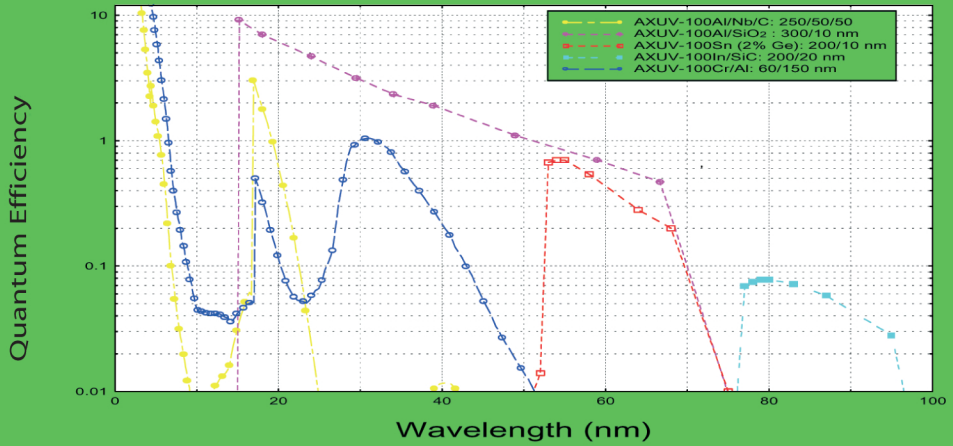
AXUV/SXUV Photodiodes with 13 nm Integrated Filters

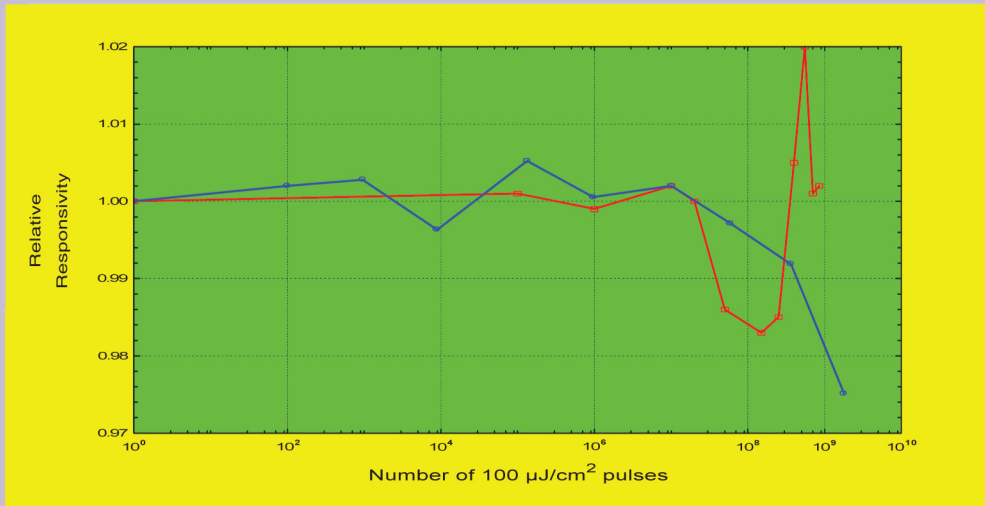


Representative AXUV photodiodes With Integrated Filters

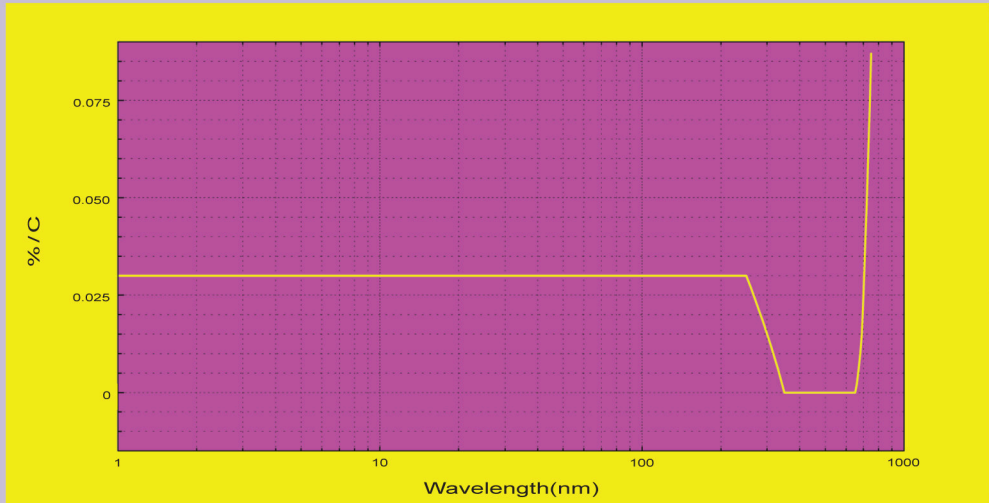


Representative AXUV Photodiodes with Integrated Filters

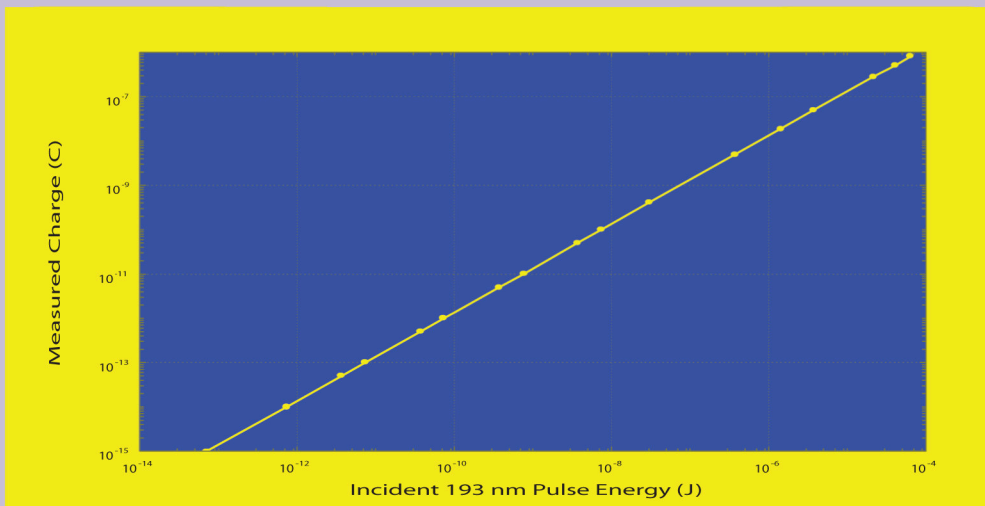




Responsivity Stability of SXUV Series Photodiodes After Exposure to 193 nm and 157 nm Excimer laser: -193 nm, -157 nm



Change in the SXUV and AXUV photodiode responsivity with temperature



Transfer Function of SXUV100RPD Diode with PA100 Amplifier

Developed in collaboration with NIST, PTB, NIH, NOAA, LANL

